https://doi.org/10.1070/RCR5034

Targeted nuclear medicine. Seek and destroy

Vladimir M. Tolmachev,[a, b] Vladimir I. Chernov,[b, c] Sergey M. Deyev [b, d]

[a] *Department of Immunology, Genetics and Pathology, Uppsala University, P.O. Box 256, SE-751 05, Uppsala, Sweden*
[b] *Research Centrum for Oncotheranostics, Research School of Chemistry and Applied Biomedical Sciences, Tomsk Polytechnic University prosp. Lenina 2, stroenie 33, 634050 Tomsk, Russian Federation*
[c] *Cancer Research Institute, Tomsk National Research Medical Center, Russian Academy of Sciences, Kooperativnyi per. 5, 634009 Tomsk, Russian Federation*
[d] *Shemyakin and Ovchinnikov Institute of Bioorganic Chemistry, Russian Academy of Sciences, ul. Miklukho-Maklaya 16/10, 117997 Moscow, Russian Federation*

The targeted delivery of radionuclides to tumours holds great promise for diagnosis and treatment of malignant neoplasms. The development of scaffold proteins has significantly simplified the design of targeting agents with desirable properties. This review comprehensively describes the key aspects of the design of radionuclide compounds, including classification of radionuclides, methodology for their attachment to targeting agents and characteristics of these agents that affect their behaviour in the body. Various targeting molecules are compared in terms of their ability to specifically find malignant foci in the body. The most recent achievements of cancer theranostics that aim at increasing the selectivity of antitumour effect are described, such as the fusion of targeting scaffold proteins with the albumin-binding domain and pretargeting. Special attention is paid to the creation of targeted radionanomaterials. Advantages and disadvantages of different strategies are analyzed and approaches for improving the delivery to tumours and for minimizing the undesirable impact on healthy organs and tissues are proposed. Particular emphasis is placed on the results of studies published in 2020–2021 that have not yet been covered by reviews.
The bibliography includes 191 references.

Contents

1. Introduction 1
2. Fundamentals of radionuclide imaging 2
3. Fundamentals of radionuclide therapy 3
4. Fundamentals of radiolabelling of targeting proteins 5
5. Current problems of the targeted radionuclide imaging and therapy 6
6. Scaffold proteins as a new type of targeting molecules for imaging 7
   6.1. Clinical use of scaffold proteins for imaging 9
   6.2. Radiopharmaceuticals for the radionuclide therapy based on scaffold proteins 10
   6.3. Pretargeting 10
   6.4. Effect of the labelling chemistry on the biodistribution of scaffold proteins and their imaging properties 11
7. Targeted radionanobioconjugates 13
8. Conclusion 16
9. List of acronyms 17
10. References 17

1. Introduction

The increase in the efficiency of treatment of disseminated malignant tumours is closely related to the active use of targeted drugs. The mechanism of delivery of these drugs is based on specific recognition of molecular anomalies typical of neoplasms, which are expressed on tumour cells and various components of the tumour stroma, including the tumour neovasculature. The main class of modern targeted anticancer therapeutic agents are monoclonal antibodies. They block the interaction between the aberrantly expressed receptors on the cell surface and their ligands or remove the camouflage of tumour cells and thus allow the immune system to recognize them.[1] Yet another type of targeted drugs are tyrosine kinase inhibitors. These compounds block signal transduction of receptor tyrosine kinases over-expressed in some malignant neoplasms. The targeted delivery is meant for transporting toxins,[2–4] drugs,[5, 6] diagnostic reagents and cytotoxic radionuclides[7, 8] into tumour cells.

It should be noted that tumours of the same origin can either express or not express a particular molecular target; therefore, not all tumours respond to the targeted therapy. Therefore, the key precondition for the successful treatment of malignant neoplasms is to reveal patients whose tumours express the target that can be attacked by a targeted drug and, hence, they will respond to the therapy with high probability. An example of such molecular target is the human epidermal growth factor receptor type 2 (HER2). Overexpression of this receptor is an indication for targeted therapy in breast and gastric cancers.[9, 10] The use of HER2-targeting drugs (the monoclonal antibody trastuzumab, its

Received 16 July 2021
© 2022 Uspekhi Khimii, ZIOC RAS, Russian Academy of Sciences and IOP Publishing Limited

conjugate with cytotoxic DM1 agent, and tyrosine kinase inhibitor lapatinib) markedly increased the survival rate of patients with these types of cancer.[9,11–13] However, high level of HER2 expression needed for efficient targeted therapy is found only in some breast cancer patients (~20%)[14] and gastric cancer patients (20–30%).[10] The decisive criterion for prescription of the targeted therapy is accurate determination of the exact HER2 level in the neoplasms.

Currently, the molecular profiling of tumours is based mainly on the analysis of biopsy material. The main drawback of the biopsy is that the procedure is invasive. Furthermore, in some cases, the anatomical location of the tumour and metastases precludes the possibility of taking tumour samples for analysis. The diagnostic value of methods based on the biopsy is reduced by the tumour heterogeneity.[15,16] During the therapy, expression of some receptors can also change due to the clonal evolution of the tumour.[17] Repeated tissue biopsy for tumour typing is rarely performed in the routine clinical practice. The drawbacks listed above are not inherent in so-called liquid biopsy method based on identification of mutations in the circulating tumour DNA. However, the applicability of this method for the molecular profiling of the tumour is restricted due to the absence of anatomical landmarks. When there are synchronous metastases with different levels of tumour expression, those that do not express this target remain unidentified.

The use of radionuclide molecular imaging improves the identification of molecular targets in tumours *in vivo*, because these methods are free from the drawbacks of tissue and liquid biopsies.[18] They can be used to select patients for the targeted therapy. In addition, monitoring of changes in the molecular target expression during the treatment can be used to evaluate the response to the applied therapy. Thus, methods of radionuclide molecular imaging allow for more personalized therapy of malignant neoplasms and, hence, make the therapy more efficient.

This review gives an integrated account of all key aspects of the creation of targeted radiolabelled compounds, ranging from classification of radionuclides, chemistry of radionuclide labelling of targeting agents and characteristics of agents that affect their behaviour in the body to the results of clinical trials of radiopharmaceuticals. A special emphasis is placed on new trends in this area and results of most recent studies that have not been covered by reviews published to date.[18–21]

V.M.Tolmachev. PhD (Medical Sciences), Professor of the Department of Immunology, Genetics and Pathology, Uppsala University; head of the Research Center Cancer Theranostics, TPU.
E-mail: vladimir.tolmachev@igp.uu.se
Current research interests: radiochemistry, radionuclide diagnosis, radionuclide therapy, molecular design of targeted agents based on scaffold proteins.
V.I.Chernov. Doctor of Medical Sciences, Professor, Deputy Director for Science and Innovations of the Tomsk NRMC, Head of the Department of Radionuclide Diagnosis of the Cancer Research Institute, TPU.
E-mail: chernov@tnimc.ru
Current research interests: radiopharmacy, radionuclide diagnosis, radionuclide therapy, theranostics.
S.M.Deyev. Academician of the RAS, Professor, Doctor of Biological Sciences, Head of the Laboratory of Molecular Immunology, IBC RAS.
E-mail: biomem@mail.ru
Current research interests: theranostics, nanobiotechnology, bioengineering of antibodies and non-immunoglobulin scaffold proteins, fabrication of targeted drugs based on biological toxins, antibiotics, photosensitizers, and radionuclides.

Translation: Z.P.Svitanko

2. Fundamentals of radionuclide imaging

Radionuclide imaging is based on external detection of the electromagnetic radiation of radionuclides injected into the human body. This radiation may consist of gamma-quanta emitted by radionuclides, which decay by isomeric transition or electron capture. In addition, it is possible to detect antiparallel photons with an energy of 511 keV, which are formed upon annihilation of the positron emitted by the radionuclide. Accordingly, depending on the source, two different principles are used to generate the image.[8]

Single gamma-quanta are detected by a gamma-camera. In this case, a collimated detector makes it possible to obtain a single projection image. Recording a multitude of such projections made at different angles around a patient provides three-dimensional image of distribution of the radionuclide in the human body. This type of imaging is called single-photon emission computed tomography (SPECT). The radionuclides that are most often used in SPECT are summarized in Table 1. It is noteworthy that ~80% of SPECT images have been obtained using ^{99m}Tc. This radionuclide is formed in the ^{99}Mo/^{99m}Tc generator and, hence, it is rather readily available and cheap. Since the half-life of this radionuclide is 6 h, the images can be obtained on the day of injection; however, imaging 24 h after injection of the nuclide is also possible. Modern SPECT scanners are optimized towards generation of ^{99m}Tc-based images. The energy of gamma-quanta from ^{123}I is also quite applicable for SPECT; however, this radionuclide is produced using cyclotrons and is much more expensive than ^{99m}Tc. Nevertheless, it is sometimes used to label proteins. The long-lived ^{111}In isotope is of interest for the radionuclide diagnosis in those cases where SPECT imaging must be carried out several days after the injection, *e.g.*, in the case of labelled full-length antibodies. The ^{67}Ga and ^{201}Tl radionuclides have a non-optimal radiation spectrum and are used only in some clinical cases where their biological and chemical properties have a crucial importance for diagnosis.

Annihilation radiation can be registered by means of the coincidence circuit using detectors that encircle the patient's body. The simultaneous detection of these quanta helps to determine the line along which annihilation took place. Processing of the information obtained upon multiple detections can be used to reconstruct the distribution of radioactivity. This principle is utilized in positron emission tomography (PET). The PET method is traditionally associated with the use of short-lived biogenic radionuclides

Table 1. Radionuclides used most often for SPECT and planar gamma-scintigraphy.[8]

Radionuclide	Half-life ($T_{1/2}$), h	Predominant energy of gamma-quanta, keV (yield)
^{67}Ga	78.3	93.3 (39%), 185 (24%), 300 (17%)
^{99m}Tc	6	140.5 (89%)
^{123}I	13.2	159 (83%)
^{111}In	67.2	171 (90%), 245 (94%)
^{201}Tl	73	167 (10%)

Table 2. Short-lived radionuclides for PET.[8]

Radionuclide	Half-life	Positron yield upon the decay (%)
^{15}O	122 s	99.9
^{13}N	9.97 min	99.8
^{11}C	20.39 min	99.8
^{18}F	109.8 min	96.7

(Table 2). These nuclides make it possible to label biologically active organic molecules without changing their chemical and biological properties. Thus, PET is a unique tool for *in vivo* studies of biochemical processes and their disorders associated with various diseases.[22]

The main physical features of PET scanning ensure a number of advantages of this method over SPECT. The PET method provides a higher sensitivity of the detection of radiation, a better spatial resolution and a higher accuracy of determination of radioactivity concentration *in vivo*. These advantages account for the preferred use of PET for imaging of pathological processes using both relatively small biologically active molecules and labelled polypeptides, first of all, monoclonal antibodies.[23,24] This is a reliable tool for the development of new targeted therapeutic agents[25,26] and for clinical imaging of tumours in order to stratify patients into risk groups.[27,28] It is noteworthy that the pharmacokinetics of full-length monoclonal antibodies is rather slow, and four to seven days after their injection are required to obtain a satisfactory contrast of the image.[29,30] It is evident that the radionuclides described in Table 2 have a very short half-life and are inapplicable for this purpose. For solving this problem, techniques for the production of some positron-emitting radionuclides with different half-lives and different chemical properties were developed (Table 3). The most important event was the commencement of industrial production of long-lived ^{89}Zr ($T_{1/2}$ = 3.27 days),[31] which is still the cornerstone of the immuno-PET involving targeting antibodies. However, other targeting proteins are also used now, such as antibody fragments and non-immunoglobulin polypeptides.[20] The optimal time of imaging for these compounds may be much shorter. Therefore, the availability of positron emitters with a half-life ranging from several hours to several days is an important precondition for the development of targeted radiopharmaceuticals.

3. Fundamentals of radionuclide therapy

The targeted delivery of cytotoxic radionuclides (beta- or alpha-emitters) into the tumour holds great promise for the treatment of malignant neoplasms.[32] Owing to the short range of alpha- and beta-particles and Auger electrons, the absorbed dose can be concentrated in the tissue immediately surrounding the site of decay, without irradiation of normal tissues remote from the tumour. The radionuclide cancer therapy has two advantages over the use of toxins or chemotherapeutic agents:

— crossfire effect (where the nuclides delivered to a cancer cell irradiate also the neighbouring cells, which makes targeting into each tumour cell unnecessary and overcomes the tumour heterogeneity in expression of the target);

— the absence of multiple drug resistance.

Table 3. Positron-emitting nuclides for labelling of the targeting proteins.[24]

Radionuclide	Half-life, h	Decay [(yield (%)]	Main gamma-radiation, keV (yield,%) [a]
^{11}C	0.34	β^+	
	Short-lived positron emitters (the image is obtained on the day of injection)		
^{94m}Tc	0.87	β^+ (70)	511 (140), 871 (94), 1868 (5.7)
		EC (30)	
^{68}Ga	1.14	β^+ (89)	511 (178), 1077(3.0)
		EC (17)	
^{75}Br	1.61	β^+ (76)	511 (152),141 (6.6), 286 (88)
		EC (24)	
^{110m}In	1.15	β^+ (62)	511 (124), 658 (98)
		EC (38)	
^{18}F	1.83	β^+ (97)	511 (194)
^{45}Ti	3.08	β^+ (85)	511 (170), 719 (0.15)
		EC (15)	
^{61}Cu	3.4	β^+ (61)	511 (122), 283 (12.5),
		EC (39)	656 (10.7), 1185 (3.7)
^{44}Sc	3.93	β^+ (94)	511 (188), 1157 (100)
		EC (6)	
	Medium-lived positron emitters (the image is obtained 24 h after the injection)		
^{66}Ga	9.49	β^+ (57)	511 (114), 834 (6.0),
		EC (43)	1039 (37.9), 2752 (23.2)
^{64}Cu	12.7	β^+ (18)	511 (36), 1346 (0.5)
		β^- (37)	
		EC (24)	
^{86}Y	14.7	β^+ (33)	511 (66), 443 (16.9), 628 (32.6),
		EC (67)	646 (9.2), 703 (15.4), 778 (22.4), 1077 (82.5), 1153 (30.5), 1854 (17.2), 1920 (20.8)
^{76}Br	16.2	β^+ (54)	511 (108), 559 (74), 657 (15.9),
		EC (46)	1216 (8.8), 1854 (14.7), 2391 (4.7), 2792 (5.6), 2950.5 (7.4)
^{55}Co	17.53	β^+ (76)	511 (152), 477 (20.2), 931 (75),
		EC (24)	1317 (7.1), 1408 (16.9)
^{72}As	26.0	β^+ (88)	511 (176), 630 (7.9), 834 (80)
		EC (12)	
	Long-lived positron emitters (the image is obtained several days after the injection)		
^{71}As	64	β^+ (30)	511 (60), 175 (83.1)
		EC (70)	
^{89}Zr	78.4	β^+ (23)	511 (46), 909 (100)
		EC (77)	
^{124}I	100.2	β^+ (23)	511 (46), 603 (61),
		EC (77)	723 (9.96), 1691 (10.4)
^{52}Mn	134.2	β^+ (30)	511 (60), 744 (90),
		EC (70)	936 (95), 1434 (100)
^{48}V	383	β^+ (50)	511 (100), 944 (7.8),
		EC (50)	983 (100), 1312 (98)
^{74}As	426.5	β^+ (29)	511 (58), 596 (59), 635 (15.4)
		β^- (34)	

Note. EC is electron capture. [a] Energies of annihilation photons are underlined.

The following requirements are imposed on therapeutic nuclides:[33]

— the amount of emitted alpha- or beta-particles or Auger electrons should be sufficient for the cytotoxic effect to be attained;

— emission of low-energy gamma-quanta with an energy of 100 – 200 keV and with a low yield for dosimetry of a particular patient (high yield of high-energy gamma-quanta is a drawback due to irradiation of normal tissues remote from the tumour);

— the desirable half-life is 1 to 14 days (the optimal half-life depends on the kinetics of the particular targeting compound);

— the chemical properties should allow stable labelling under mild conditions;

— the radioactive metabolites of the labelled protein should be rapidly excreted.

Currently, the therapeutic radionuclides that are used most often are beta-emitters. Theoretical calculations show that the antitumour effect of the beta-emitting radionuclides depends on the tumour size and beta-particle energy.[34–37] Nuclides that emit high-energy beta-particles are most efficient for the treatment of large tumours. Due to the long range of these particles in tissues, they irradiate the parts of the tumours that cannot be entered by radiopharmaceuticals due to poor vascularization or possible heterogeneity of expression of the molecular target. However, high-energy beta-particles are unsuitable for the treatment of single malignant cells or micrometastases. The greater part of their energy is spent for devastating impact outside the tumour cells, *i.e.*, in normal tissues. Conversely, low-energy beta-particles release their energy in close vicinity of the site of decay. The crossfire effect in moderate in this case, and the efficiency of nuclides emitting low-energy beta-particles can be insufficient for large tumours. However, such nuclides can affect subclinical tumours, which cannot be detected by modern diagnostic methods. For this reason, the interest in nuclides that emit beta-particles with a lower energy, such as ^{177}Lu, ^{161}Tb and ^{67}Cu, has increased in recent years. In the ideal case, the radionuclide should be chosen depending on the size of the tumour to be treated. The physical properties of some beta-emitting nuclides potentially suitable for radionuclide therapy are listed in Table 4.

Alpha-emitting nuclides are highly promising for radionuclide therapy.[41] They have high cytotoxicity, and their action does not depend on the oxygenation of tumour cells. Several hits of alpha-particles into the cell nucleus are sufficient to destroy the tumour cell. The alpha-particle has a relatively short range — approximately 10 cell diameters, which makes it possible to avoid irradiation of normal tissues surrounding the tumour. Thus, alpha-emitters can be used to treat minor remainders of tumour tissue, micrometastases and, possibly, single circulating tumour cells. The main problem faced by targeted alpha-therapy is that only a few radionuclides can be obtained by economically justified methods: ^{211}At ($T_{1/2}$ = 7.2 h), ^{212}Bi ($T_{1/2}$ = 1.0 h), ^{213}Bi ($T_{1/2}$ = 0.75 h), ^{223}Ra ($T_{1/2}$ = 11.4 days), ^{225}Ac ($T_{1/2}$ = 10 days) and ^{227}Th ($T_{1/2}$ = 18.7 days) (Table 5). In addition, some physical and chemical properties of the above radionuclides prevent their wide clinical use. For example, ^{223}Ra proved to be useful for the treatment of bone metastases, but its chemical properties are inapplicable for labelling of targeting molecules. The half-lives of ^{212}Bi and ^{213}Bi are too short to ensure an efficient systemic therapy; however, they can hopefully be effective in the case of topical administration.

Table 4. Physical properties of some beta-emitting nuclides potentially suitable for targeted radionuclide therapy.[38–40]

Nuclide	Half-life, days	Average energy of beta-radiation, MeV	Mean range, mm	Photon energy, keV (yield)
		Low-energy beta-emitters		
^{67}Cu	2.6	0.141	0.71	91 (7%)
				93 (16%)
				185 (49%)
^{131}I	8.0	0.181	0.91	364 (82%)
^{161}Tb	6.9	0.154	0.77	75 (10%)
^{177}Lu	6.7	0.133	0.67	113 (6%)
				208 (11%)
		Medium-energy beta-emitters		
^{77}As	1.6	0.228	1.2	–
^{153}Sm	1.9	0.229	1.2	103 (30%)
^{186}Re	3.7	0.362	1.8	137 (9.4%)
		High-energy beta-emitters		
^{188}Re	0.71	0.764	3.5	155 (15%)
^{166}Ho	1.1	0.666	3.2	80.5 (6.7%)
^{90}Y	2.7	0.935	3.9	–
^{76}As	1.1	1..0	5.0	559 (45%)
				657 (6.2%)

Note. Photons with > 5% yields are presented.

Table 5. Alpha-emitting nuclides potentially suitable for targeted radionuclide therapy.[42]

Radionuclide in the decay chain	Half-life	Decay
^{211}At	7.2 h	α (42%)
		EC (58%)
^{211}Po	0.52 s	α (100%)
^{207}Bi	39 years	
^{207}Pb	Stable	
^{225}Ac	9.9 days	α (100%)
^{221}Fr	4.9 min	α (100%)
^{217}At	32 ms	α (99.98%)/β$^-$ (0.01%)
^{213}Bi	45.6 min	α (2%)/β$^-$ (98%)
^{213}Po	4.2 μs	α (100%)
^{209}Pb	3.3 h	β$^-$ (100%)
^{209}Bi	Stable	
^{227}Th	18.7 days	α (100%)
^{223}Ra	11.4 days	α (100%)
^{219}Rn	4.0 s	α (100%)
^{215}Po	1.8 ms	α (100%)
^{211}Bi	2.2 min	α (99.7%)/β$^-$ (0.3%)
^{207}Tl	4.8 min	β$^-$ (100%)
^{207}Pb	Stable	
^{212}Pb	10.6 h	β$^-$ (100%)
^{212}Bi	60.6 min	α (36%)/β$^-$ (64%)
^{208}Tl	3.0 min	β$^-$ (100%)
^{212}Po	0.3 μs	α (100%)
^{208}Pb	Stable	

Daughter radionuclides represent one more serious problem of the therapeutic use of alpha-emitting radionuclides.[42] During the decay, the nucleus acquires so-called recoil energy, which exceeds the chemical bond energy. This

is accompanied by cleavage of the bond between the targeted protein and the daughter nuclide; as a result, the latter is redistributed in the body in accordance with its chemical properties. If the daughter nuclide has a short half-life, this may become a problem. For, example, the activity of ^{221}Fr is equal to the half of activity of the injected ^{225}Ac as soon as 4.9 min (^{221}Fr half-life) after the injection. The use of radionuclides that decay to give long-lived daughter nuclides could be a possible solution to this problem. For example, the formation of long-lived ^{223}Ra (the daughter nuclide of ^{227}Th) occurs much more slowly. One more possible solution is encapsulation of the alpha-emitting radionuclides into liposomes, which prevent them from getting into the blood stream.[42]

The physical properties of ^{211}At are more suitable for systemic radiotherapy, but only when pretargeting or short peptides are used. The short half-life of ^{211}At precludes the transportation of this nuclide over long distances; however, it is considered to be promising for the use in dedicated cyclotron-based therapy centres[43] organized similarly to PET centres.

4. Fundamentals of radiolabelling of targeting proteins

The strategy of radioactive labelling of targeting proteins includes the choice of radionuclide, chelator or linker for its conjugation to the protein and the choice of an approach for purification of the radiolabelled protein. In addition, development of the labelling procedure includes the choice of the buffer (composition, pH, molar concentration) for binding chelators or linkers and the solvent (considering lipophilicity and composition) for purification.

It is evident that the optimal labelling should comply with the following requirements:

— stable binding of the radionuclide to the protein *in vivo*;

— preservation of the secondary and tertiary structures of the targeting protein;

— preservation of the protein affinity for its molecular target;

— preservation of the biodistribution of the protein;

— good intracellular retention of the radioactive catabolites in the case of fast protein internalization by tumour cells after binding;

— fast excretion of radioactive metabolites from the body.

Stability of the compound depends on the approach to radiolabelling. Labelling using radioactive halogens (^{18}F, iodine and bromine radioisotopes, ^{211}At) occurs *via* covalent bond.[44] This bond is chemically stable *in vivo* if there is no enzymatic system able to cleave it. The terms 'deiodination' and 'defluorination', *i.e.*, release of free iodide or fluoride reflect mainly the results of intracellular degradation of radiolabelled proteins after internalization into the tumour cells that express the target, normal tissues or excretory organs (kidneys and liver). Conversely, radiometal labelling using bifunctional chelators is always reversible. In addition, chelating properties are inherent in some blood proteins. When they are present in blood in excess over the labelled proteins, the radiometal label may split off. For example, transferrin usually provides iron transport, but can also strongly bind various trivalent radiometals. The interaction of an antibody labelled with ^{111}In by means of a chelator, cyclic anhydride of diethylenetriaminepentaacetic acid (CDTPA), with transferrin results in transchelation of 9% of the label per day to transferrin.[45] Similarly, oxotechnetium complexes can be affected by peptides containing a free thiol group.[45] Thus, the complex of a radiometal with a chelator should possess both high thermodynamic stability and kinetic inertness.

The use of macrocyclic chelators is one of the approaches used to solve the problem of stability of radiometal labels.[46–48] The spatial configuration of the chelators is favourable for the complex formation with metal ions, which minimizes the structural rearrangements during the chelation and reduces the entropy penalty .[49] It is important to note that metal complexes with macrocyclic chelators are kinetically inert, and their dissociation rate is low. This inertness of macrocyclic chelators turns into low rate of their association during complex formation; therefore, for fast labelling, heating to 60–95 °C is often required. These labelling conditions are usually suitable for short peptides,[50–52] but in the case of antibodies, this approach is inadmissible due to their denaturation. Nevertheless, the use of macrocyclic chelators with gentle heating (~37 °C) is possible even for monoclonal antibodies.[53–55]

1,4,7,10-Tetraazacyclododecane-1,4,7,10-tetraacetic acid (DOTA) is the most versatile and, hence, the most popular macrocyclic chelator (Fig. 1). This chelator is suitable for labelling using a broad range of radiometals applicable for SPECT (for example,^{111}In)[56] and PET [^{55}Co (Ref. 57),^{44}Sc (Ref. 58) and ^{68}Ga (Ref. 59)] and also for radionuclide therapy [^{47}Sc (Ref. 60), ^{177}Lu (Ref. 61), $^{212/213}$Bi (Ref. 62), ^{212}Pb (Ref. 63), ^{225}Ac (Ref. 64) and ^{227}Th (Ref. 65)]. Several DOTA derivatives that are capable of binding to the amino groups of lysine residues and to the thiol groups of cysteine residues of proteins are commercially available (see Fig. 1), which promotes their application. This versatile chelator forms thermodynamically stable and kinetically inert complexes with the metals listed above. The labelling involving

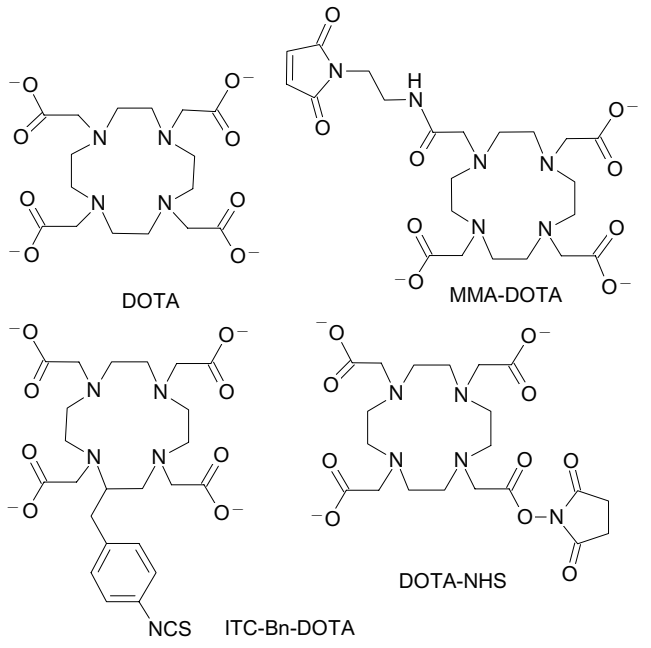


Figure 1. Structures of the macrocyclic DOTA chelator and its derivatives: MMA-DOTA (reacts with the SH group), ITC-Bn-DOTA and DOTA-NHS (reacts with the NH_2 group).

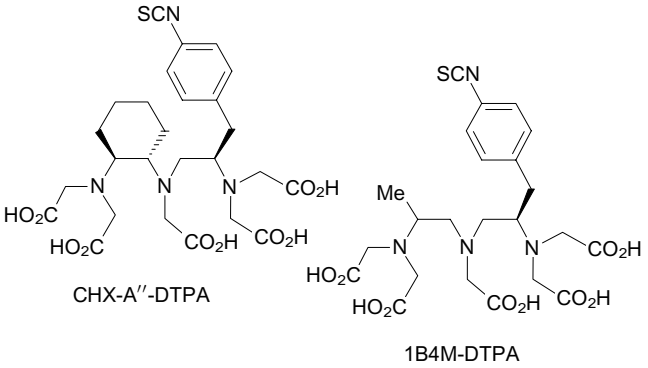


Figure 2. Structures of CHX-A″-DTPA and 1B4M-DTPA (tiuxetan).

DOTA requires heating and may be unsuitable for targeting molecules based on immunoglobulins.

The use of acyclic semi-rigid chelators, diethylenetriaminepentaacetate (DTPA) derivatives such as CHX-A″-DTPA and 1B4M-DTPA (tiuxetan) (Fig. 2) can serve as alternatives to macrocyclic chelators for some radionuclides. The rate of labelling using these chelators is much higher. On the other hand, the inclusion of additional groups into the DTPA backbone restricts the freedom of vibrations and rotations of components, which decreases the entropy penalty during complexation. This, in turn, increases the stability of the compound. The 1B4M-DTPA chelator ensures a reasonable stability of proteins labelled with ^{177}Lu (Ref. 66) and ^{90}Y (Ref. 67). The monoclonal antibody ibritumomab in combination with tiuxetan as the chelating agent labelled with ^{90}Y using 1B4M-DTPA is successfully employed for the therapy of lymphoma.[68, 69] The CHX-A″-DTPA chelator provides a very high stability *in vivo* for labelling of proteins with ^{111}In (Ref. 70), ^{177}Lu (Ref. 71) and $^{90/89}$Y (Refs 72 and 73).

Currently ^{89}Zr is the only positron-emitting radiometal suitable for immuno-PET with full-length monoclonal antibodies. Radiolabelling of monoclonal antibodies for preclinical and clinical studies has so far been mainly accomplished using derivatives of the DFO chelator (DFO is desferroxamine, trade mark Desferal®) (Fig. 3). The main advantage of this chelator is the possibility of efficient ^{89}Zr labelling of immunoglobulins at neutral pH and room temperature. However, the main drawback of hexadentate chelators meant for binding eight-coordinate Zr^{4+} is relatively low stability of the resulting complex.[74] For example, the use of ^{89}Zr for the labelling of trastuzumab, an anti-HER2 antibody, led to a considerably higher accumulation of the radionuclide in the liver and the bones in comparison with the use of ^{111}In.[75] This may complicate the imaging of often encountered liver and bone metastases. The octadentate derivatives of DFO reported by van Dongen and co-workers[76] and Denat and co-workers[77] are free from this drawback.

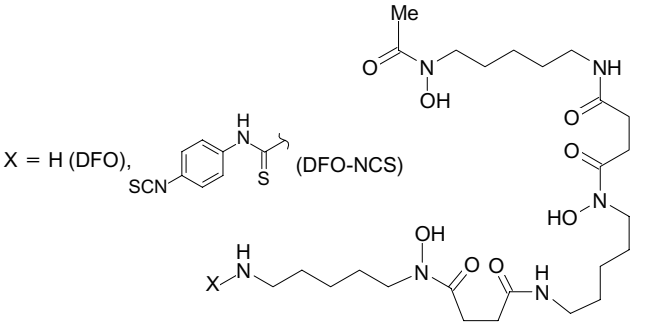


Figure 3. Structures of DFO and its isothiocyanate derivative (DFO-NCS).

It should be emphasized that the choice of the optimal labelling strategy should take into account the rate of internalization of the peptide after its binding to the molecular target both in the tumour cells and in normal tissues (if the target is present in them) and the liver and kidney uptake of the polypeptide.[44] After internalization of the protein *via* receptor-mediated endocytosis, endosomes fuse with lysosomes in the cell cytoplasm in which the transported proteins undergo proteolytic cleavage under the action of enzymes. If radioactive metabolites are charged or polar, they remain inside the cells. The labels formed by these radiometabolites are called residualizing labels. Most often (but not always), residualizing labels are formed by radiometals. If the radioactive metabolites are lipophilic, they can diffuse through lysosome membranes and cytoplasmic membrane and exit from the cells. Such labels are called non-residualizing labels. The labels formed by radioactive halogens usually belong to this type. The bivalent binding of antibodies to tumour cells often induces relatively fast internalization of more than a half of cell-bound radioactivity per day.[78] The use of non-residualizing labels is accompanied by leakage of radiometabolites from tumours and low general retention level of radioactivity by the tumour. Thus, radiometals are preferred for labelling of antibodies.

5. Current problems of the targeted radionuclide imaging and therapy

The key condition for the successful use of labelled compounds in clinical oncology is high sensitivity and specificity of tumour imaging. These characteristics, in turn, depend on the ratio of radioactivity levels in the tumours and in surrounding tissues. Currently, radionuclide imaging of molecular targets is carried out using labelled monoclonal antibodies and their derivatives.[79] Development of this field resulted in the creation of labelled molecules for targeted delivery with good specificity and high binding affinity. The main drawback of full-length antibodies is their large size, which leads to slow clearance, extravasation and unsatisfactory penetration into the tumour.[80] These features decrease the contrast of the image; in addition, the diagnostic imaging can be carried out only several days after the injection. Furthermore, non-specific tumour accumulation of radiopharmaceuticals with a molecular mass above 45 kDa decreases the specificity of molecular imaging with full-length antibodies.[80]

The radionuclide therapy involving labelled antibodies proved to be highly efficient in the treatment of radiosensitive haematological tumours; however, results for solid neoplasms are poor. This is due to the slow clearance of antibodies, which leads to high irradiation doses of intact tissues, including radiosensitive bone marrow.[7]

Today, only two delivery vectors showed evident clinical efficacy for the targeted radionuclide therapy of solid malignant tumours. These are somatostatin analogues and prostate-specific membrane antigen (PSMA) inhibitors, which are small-size peptides or pseudopeptides. ^{90}Y- and

^{177}Lu-DOTATATE(DOTATOC), where DOTATATE is the octapeptide D-Phe-Cys-Phe-D-Trp-Lys-Thr-Cys-Thr covalently linked to the DOTA chelator and DOTATOC is (DOTA^0-Phe^1-Tyr^3)-octreotide, are successfully used in many nuclear medical centres for the treatment of neuroendocrine tumours.[81] The top positions in the treatment of metastatic prostate cancer belong to ^{177}Lu-PSMA and ^{225}Ac-PSMA,[82,83] the theranostic pair of which for PET imaging is ^{68}Ga-PSMA.[84] The success of application of these peptides indicates that a considerable decrease in the size of the targeted molecules is a promising strategy for development of new therapeutic radiopharmaceuticals.

6. Scaffold proteins as a new type of targeting molecules for imaging

As noted above, the major problem for the clinical use of full-length antibodies is related to their large size.[7] Therefore, bioengineering design of targeted molecules of smaller size appears to be a rather promising strategy. High-affinity ligands can be obtained using a robust scaffold consisting of amino acids.[85] A considerable advantage of scaffold proteins over antibodies is their smaller size (Fig. 4).

One of the designs of such proteins called affibody[86] uses the domain scaffold of the staphylococcal protein A from the bacteria *Staphylococcus aureus*. The affibody structure consists of three alpha-helices. Helices 1 and 2 contain 13 randomized amino acids, different combinations of which allow one to select binding compounds with high affinity. Helix 3 ensures the structural stability of the affibody. Affibody became the first type of scaffold proteins dedicated to the targeted delivery of radionuclides.[87] Its small size (58 amino acids) provides for good penetration of the molecule into the tumour and fast elimination of the unbound compound from blood.[87,88] Thus, high ratio between the protein concentrations in the tumour and in the surrounding tissue is attained and, therefore, the optimal contrast of the image can be obtained within several hours after the injection.

Several types of affibody molecules possessing high affinity [dissociation constant from several pmol L^{-1} (pM) to several nM] to a number of molecular targets were selected. The targets included human epidermal growth factor receptor type 1 (HER1, or EGFR),[89–91] type 2 (HER2) [87] and type 3 (HER3),[92] insulin-like growth factor 1 receptor (IGF-1R),[93] platelet-derived growth factor receptor beta (PDGFR beta),[94] vascular endothelial growth factor receptor 2 (VEGFR2),[95] programmed cell death ligand 1 (PD-L1)[96] and carbonic anhydrase IX (CAIX).[97,98] The potential of the indicated compounds for radionuclide molecular imaging was studied.

Direct comparison of labelled HER2-binding affibody molecules and monoclonal antibodies in mouse models demonstrated that 2–6 h after the injection, affibody shows a several times higher tumour/blood distribution ratio of the label than the monoclonal antibody does 72 h after the injection (the optimal time point for imaging of these compounds).[99,100]

More information was provided by comparison of CAIX-binding affibody molecule ^{111}In-DOTA-ZCAIX:2 and ^{111}In-G250 $(Fab')_2$.[98] The $(Fab')_2$ antibody fragments are known to provide a higher contrast than intact immu-

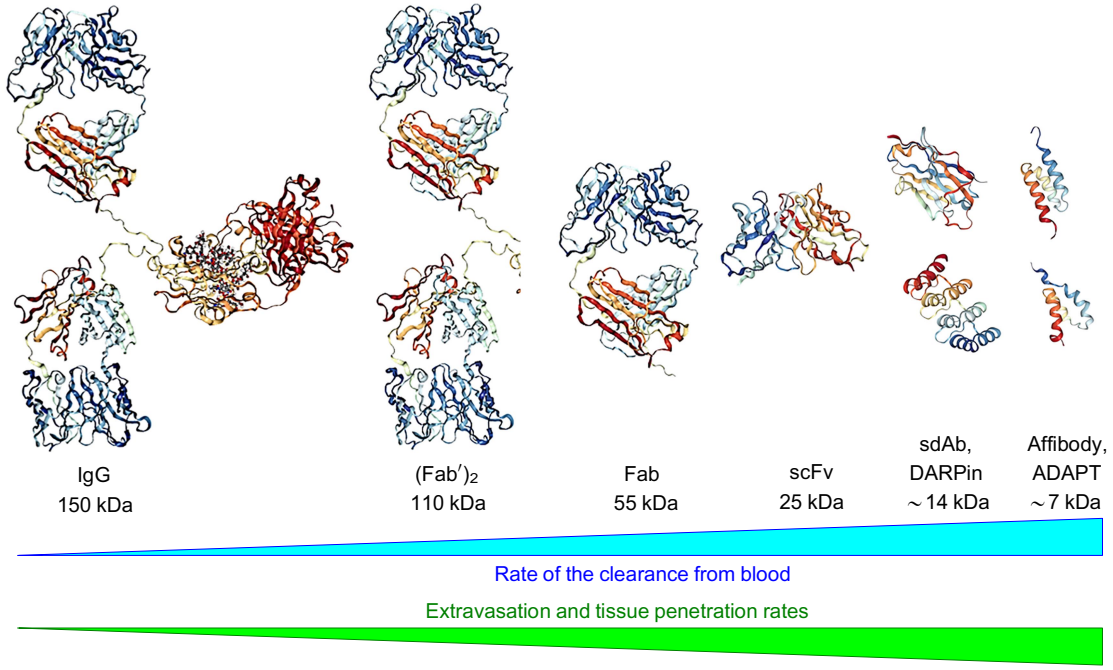


Figure 4. Targeted polypeptide vectors for radionuclide therapy and relative size of the proteins used for radioimmunodetection and molecular imaging. IgG is immunoglobulin G; $(Fab')_2$ is a fragment of immunoglobulin molecule including two antigen-binding fragment; Fab is the antigen-binding fragment of the immunoglobulin molecule composed of one constant domain and one light and heavy chain variable domain; scFv is a single chain variable fragment, which is a fusion protein from the variable regions of the heavy and light chains of the immunoglobulin molecule connected by a short linker peptide; sdAb is the single-domain antibody, also known as nanobody, which represents the variable domain of the antibody; DARPin (designed ankyrin repeat protein) is a genetically engineered scaffold protein containing 4 or 5 ankyrin repeats; affibody is a scaffold protein developed on the basis of the Z-domain of the staphylococcus protein A; ADAPT is a scaffold peptide based on albumin-binding domain of 46 amino acids of streptococcus protein G. The images were taken from the open Protein Data Bank (https://www.rcsb.org).

noglobulins, and the optimal time gap between the injection and imaging is shorter for these fragments than for antibodies.[101] The results of direct comparison in the same mouse model (Fig. 5) demonstrated that the tumour/blood distribution ratio of ^{111}In-DOTA-ZCAIX:2 four hours after the injection was 30 times higher than this value at the same time point after the injection of ^{111}In-G250 (Fab′)$_2$. Only 24 h after the injection of ^{111}In-G250 (Fab′)$_2$, the tumour/blood ratio of the nuclide content was the same as 4 h after the introduction of ^{111}In-DOTA-ZCAIX:2. Nevertheless, the tumour/lungs, tumour/liver, tumour/bones and tumour/muscles distribution ratios were markedly higher for the affibody molecule.

Direct comparison discussed above is the most accurate way of testing labelled molecules for imaging, because all factors associated with the variability of animals and xenografts from one batch to another are the same for both compounds. Comparison with published data is less accurate, but the results from some publications[20, 102, 103] convincingly demonstrate that the affibody provides a much better contrast in preclinical models than the intact antibodies or their (Fab′)$_2$, Fab or scFv fragments.

In recent years, Professor Hober's group[104] (Royal Institute of Technology, Stockholm) designed a new type of scaffold proteins, which were called ADAPT. This polypeptide is based on the albumin-binding domain consisting of 46 amino acids derived from streptococcus protein G. Its size is 25% smaller than the affibody size, which improves extravasation and increases the rate of penetration into tissues, and this, in turn, provides more efficient binding of the label to the target molecules. The ADAPT scaffold also has a three-helical structure. Currently, ADAPT with low nanomolar or subnanomolar affinities for the tumour targets (HER2 and HER3) have been developed. The applicability of labelled ADAPT for PET and SPECT imaging of HER2 was demonstrated in animal experiments.[105, 106] It was shown that the radionuclide imaging involving labelled ADAPT6 allows clear differentiation between the human xenografts with high and low HER2 expression levels.[105, 107] Further studies were devoted to optimization of the molecular design of the ADAPT6-based imaging and therapeutic molecules. In particular, it was found that the non-structured N-terminal sequence plays an important role in the structural integrity of the scaffold. The removal of this part leads to destabilization of helix 1 of the ADAPT6 polypeptide.[97] It was found that the use of N-terminal sequences GC(HE)$_3$DANS and GCVDANS substantially increases the contrast of the imaging, thus ensuring the ratio between the radionuclide concentrations in the tumour and in the blood of 395 ± 75 and 419 ± 91, respectively, for ^{111}In-labelled ADAPT6 derivatives.[97] An interesting finding is that the dimerization of ADAPT6 increases the affinity by an order of magnitude, but accumulation of dimeric forms in the tumours markedly decreases.[108] This fact is consistent with the data obtained both for the affibody[109] and for DARPin (see below).[110] In both cases, dimerization increased the affinity of drugs, but reduced their uptake by the tumour. This convincingly indicates that the small size of scaffold proteins is of primary importance. Most likely, the small size is responsible for the critical advantage in the extravasation rate, and the increase in the affinity due to dimerization cannot counterbalance the disadvantage of less efficient extravasation.

One more type of scaffold proteins, designed ankyrin repeat protein (DARPin), has a somewhat bigger size (130–160 amino acids).[85] The DARPin scaffold consists of 4 or 5 repeats, each containing 33 amino acids and including a

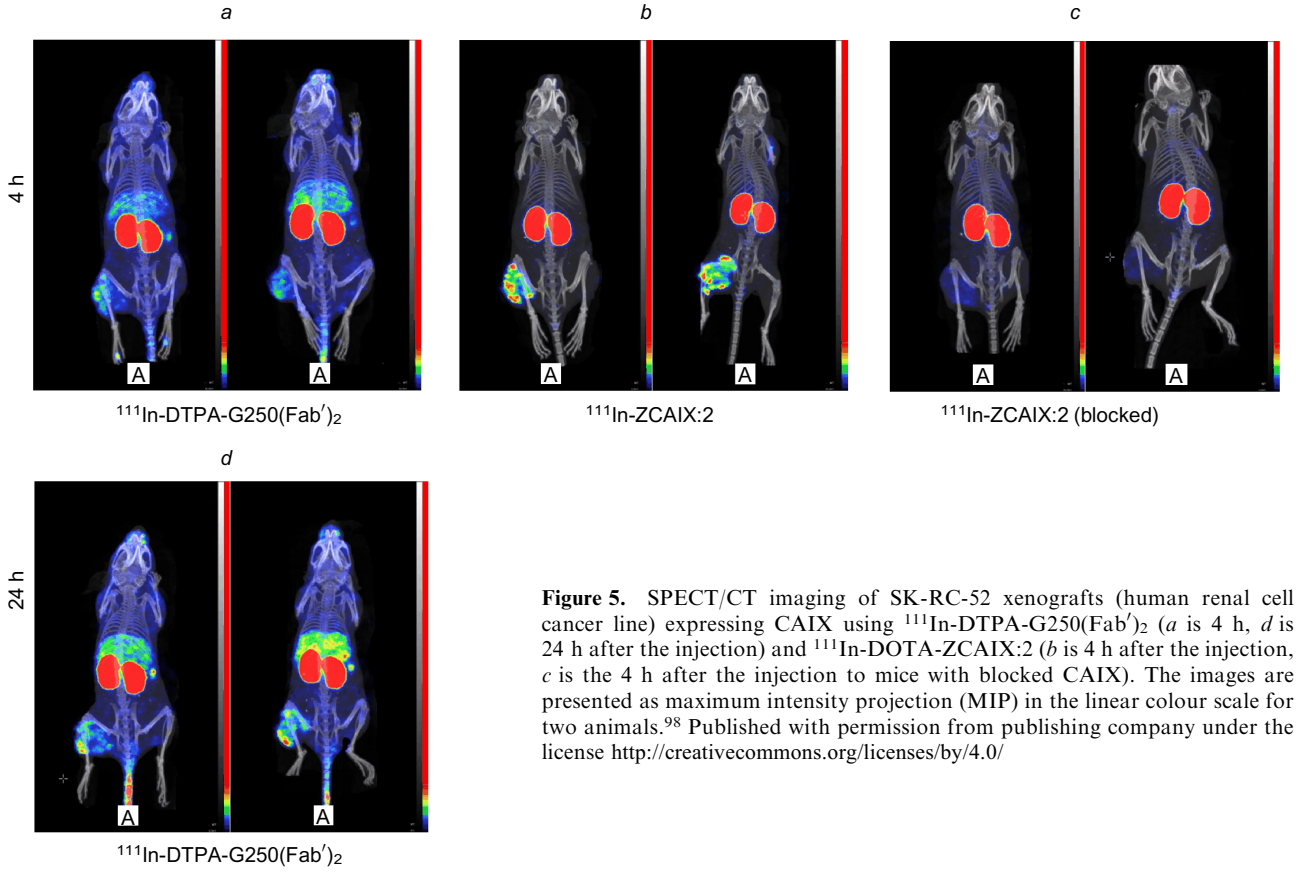


Figure 5. SPECT/CT imaging of SK-RC-52 xenografts (human renal cell cancer line) expressing CAIX using ^{111}In-DTPA-G250(Fab′)$_2$ (*a* is 4 h, *d* is 24 h after the injection) and ^{111}In-DOTA-ZCAIX:2 (*b* is 4 h after the injection, *c* is the 4 h after the injection to mice with blocked CAIX). The images are presented as maximum intensity projection (MIP) in the linear colour scale for two animals.[98] Published with permission from publishing company under the license http://creativecommons.org/licenses/by/4.0/

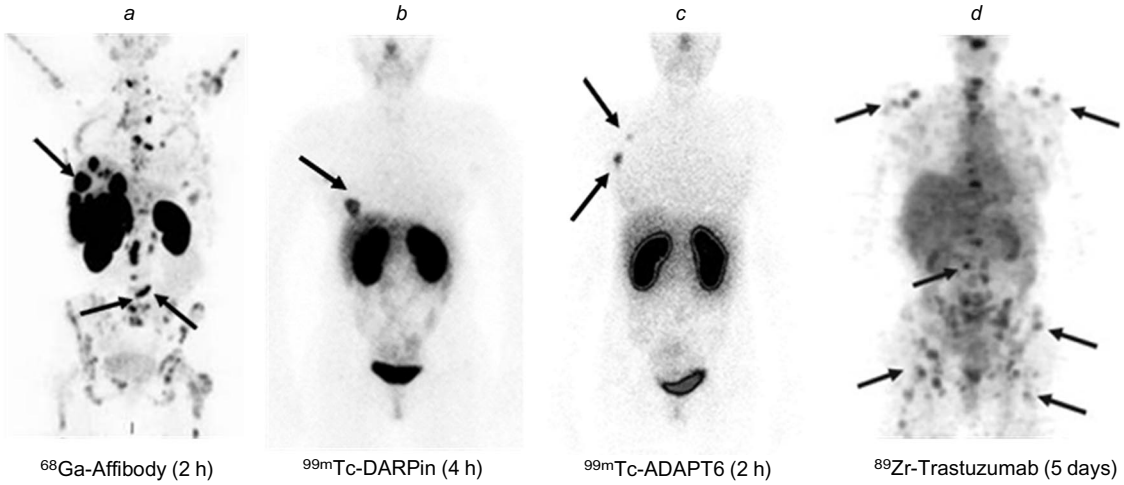


Figure 6. Imaging of the HER2 expression in breast cancer using affibodies (*a*),[123] DARPin G3 (*b*),[125] ADAPT6 (*c*)[126] and the monoclonal antibody trastuzumab (*d*).[75] The value in parentheses is the time that passed after injection of the radiopharmaceutical. Published with permission from the publishing company: Fig. *a* under the license of Creative Commons Attribution (http://ivyspring.com/terms), Figs *b*–*d* under the license of the *Journal of Nuclear Medicine*, Open Access (https://jnm.snmjournals.org/page/permissions).

beta-fold and two antiparallel alpha-helices. The DARPin protein with a subnanomolar affinity for molecular targets such as HER2,[110] EGFR (Ref. 111) and EpCAM (epithelial cell adhesion molecule, a membrane protein)[112] or with a low nanomolar affinity for HER3 (Ref. 113) is of obvious interest for molecular imaging. In the last-mentioned case, its applicability was confirmed by Goldstein *et al.*,[114] who used a mouse model and ^{111}In-labelled HER2-binding DARPin G3 containing four repeats. The authors found that such proteins are efficiently and specifically accumulated in tumours and are quickly eliminated from normal tissues.[114] Furthermore, the possibility of HER2 imaging using DARPin 9_29 containing five repeats was demonstrated.[115] According to a comparative study, DARPin G3 (4 repeats) ensures a better tumour imaging than DARPin 9_29 (5 repeats), which is probably attributable to the smaller size of the former.[116] The possibility of high-contrast imaging of EpCAM expression with DARPin Ec1 was demonstrated using a pancreatic cancer model.[117] Radioiodinated DARPin Ec1 generates a better contrast than any other agent for radionuclide imaging of EpCAM.[117] The DARPin Ec1 protein was also used for the imaging of EpCAM expression in ovarian cancer [118] and triple negative breast cancer.[119]

An important benefit of scaffold proteins is that they can be obtained by chemical synthesis or low-cost bacterial production, which makes them significantly less expensive compared to antibodies. One more advantage of these compounds is that their properties and high affinity for molecular targets are restored after thermal or chemical denaturation. This makes it possible to use high temperatures (up to 95 °C) and acidic or alkaline buffer solutions (in the pH range of 3.6–11.0) during labelling, which enhances the efficiency of the procedure.[105, 120, 121] Under these conditions, any monoclonal antibody would have been irreversibly denatured.

6.1. Clinical use of scaffold proteins for imaging

Currently, phase I and II clinical trials for a labelled anti-HER2 affibody have been completed. It was shown that its injection is well tolerated by patients, does not induce an immune response and does not cause a high radiation exposure for the examined patient.[122–124] In addition, studies confirmed the applicability of affibodies for imaging of HER2-expressing metastases (Fig. 6) and for differentiating between metastases with high and low expression of target receptors.[123] Unlike antibodies, the affibodies generate high-contrast images several hours after the injection.[122, 123] Currently, the anti-HER2 affibody is under phase III clinical trials.

Phase I clinical trials demonstrated the safety and tolerability of ^{99m}Tc-labelled DARPin G3 being injected to patients with a primary breast cancer.[103] The effective dose was found to be an order of magnitude lower than that in the case of ^{89}Zr-labelled monoclonal antibodies. It was found that the ^{99m}Tc-labelled DARPin G3 can discriminate between HER2-positive and HER2-negative tumours (see Fig. 6). The liver uptake of ^{99m}Tc-labelled DARPin G3 depended on the weight of the injected protein. At least 2 mg of the protein should be injected to suppress the HER2-specific uptake in the liver and visualize liver metastases.

The safety and tolerability of ^{99m}Tc-labelled ADAPT6 was also confirmed in phase I clinical trial[126] in which SPECT-detection of HER2 expression in the primary breast cancer and axillary metastases was performed for prescription of the neoadjuvant trastuzumab therapy. The radiation exposure caused by this imaging agent was similar to that resulting from the use of ^{99m}Tc-DARPin G3. In the case of ^{99m}Tc-ADAPT6, the amount of the injected protein was also critical. The introduction of 500 μg provided reliable differentiation between HER2-positive and HER2-negative tumours as soon as 2 h after the injection (see Fig. 6). Conversely, the injection of 250 or 1000 μg of this radiopharmaceutical did not provide such result.

For comparison, Figure 6 shows the imaging of HER2 expression in breast cancer generated using radiolabelled scaffold proteins or the monoclonal antibody trastuzumab. It is evident that scaffold proteins ensure much better contrast of the image 2–4 h after the injection than the monoclonal antibody does by the fifth day. This Figure demonstrates the obvious superiority of scaffold proteins for radionuclide molecular imaging.

6.2. Radiopharmaceuticals for the radionuclide therapy based on scaffold proteins

The major challenge arising in the development of scaffold-based radiopharmaceuticals for radionuclide therapy is high renal reabsorption of the affibody[123] and ADAPT (Ref. 105) and DARPin proteins.[116] Furthermore, usual methods for decreasing the reabsorption such as pre- or co-injection of positively charged amino acids or gelofusine (solution of succinylated gelatine) do not affect significantly this feature of tested scaffold proteins.[127–129] Nevertheless the following approaches are still applicable to decrease the uptake or retention of radionuclides by renal cells after the injection of labelled scaffold proteins:

(1) the use of non-residualizing labels,
(2) linking to albumin-binding domain (ABD),
(3) pretargeting.

After the reabsorption in kidneys, scaffold proteins are rapidly internalized and degrade in lysosomes. Metabolites of radioactive iodine are soon excreted from kidney cells, which reduces the radiation exposure of kidneys. Metabolites of radioactive metals are retained inside the cells for a long time, thus causing a high radiation exposure. The internalization of scaffolds into tumour cells is slow;[105,116,123] therefore, the rate of radionuclide extravasation from the malignant cells is rather low even when non-residualizing labels are used. It was shown that the use of non-residualizing radioiodine decreases the kidney retention of ^{131}I-labelled affibodies[33] and ADAPT[107] and DARPin[116] proteins. This opens up the way towards conjugates potentially suitable for radionuclide therapy. However, this approach is inappricable to the fabrication of therapeutic radiopharmaceuticals with ^{227}Th and ^{225}Ac alpha-emitting radiometals.

A combination of a scaffold protein with the albumin-binding domain allows the targeted molecule to reversibly react with blood albumin. The scaffold protein–ABD–blood albumin complex has a molecular mass of approximately 80 kDa, which precludes its glomerular filtration and the subsequent renal reabsorption. At the same time, this construct is approximately 2 times smaller in size than the antibody, which facilitates its extravasation and accumulation in the tumour. The utility of this approach was initially demonstrated for affibody molecules.[130–132] It enabled preventing tumours formation in the case of xenografts with a high HER2 expression.[130]

A similar approach was used to modify the distribution of ^{177}Lu-labelled HER2-binding ADAPT6.[133] The authors used an improved type of albumin-binding domain, ABD_{035}, characterized by femtomolar affinity to human albumin. It was found that the biodistribution depends on the relative positions of ADAPT and ABD_{035} in the recombinant fusion protein. The best results were attained when ABD_{035} was bound to the C-terminus of ADAPT6. In this case, the uptake of the label in kidneys decreased 14-fold. Experimental therapy (Fig. 7 *a*) showed that a single injection of ^{177}Lu-DOTA-ADAPT6-ABD_{035} in a dose of 18 MBq resulted in a considerable decrease in the tumour growth rate in comparison with the control group. The median survival rate increased from 25 days in the control group to 70 days for the group that received a single injection of 18 MBq ^{177}Lu-DOTA-ADAPT6-ABD_{035} (see Fig. 7 *b*). The effect was dose-dependent: in the case of two injections of 18 MBq of this pharmaceutical the effect was more pronounced (see Fig. 7 *a* and *b*). The therapy was well tolerated, and the weight of treated mice did not differ significantly from the weight of mice in the control group (see Fig. 7). These data, together with the results of affibody experiments,[130–132] indicate that a combination of ADAPT6 with ABD may form the basis for the development of scaffold protein conjugates for radionuclide therapy.

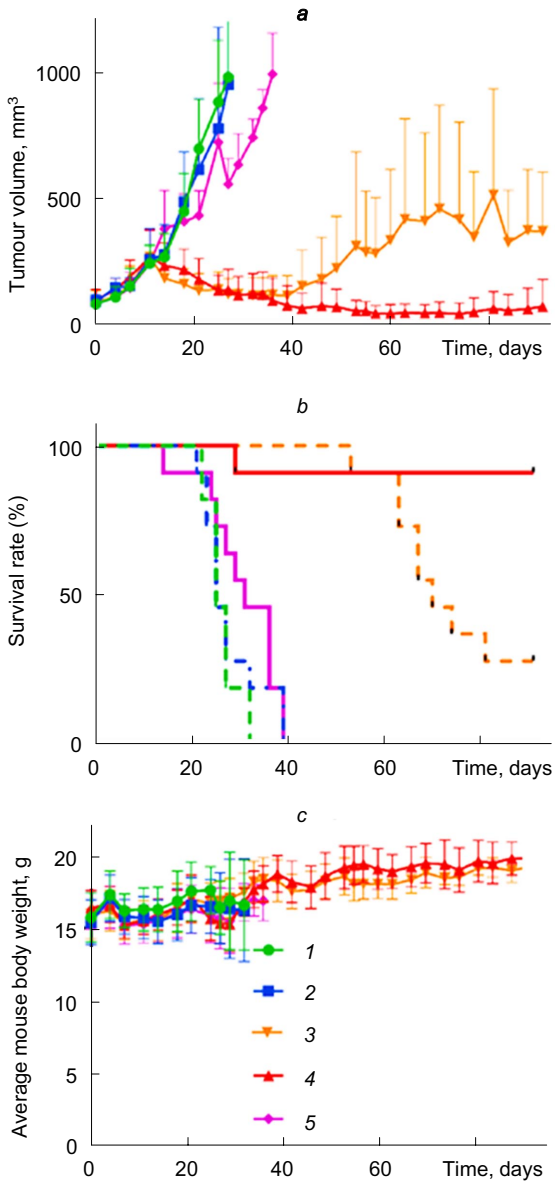


Figure 7. Results of radionuclide therapy *in vivo*: average volume of HER2-expressing SKOV-3 xenografts in thymus-deprived BALB/c mice (n = 11) (*a*), survival rate (*b*), average body weight of mice (*c*) after the administration of phosphate buffered saline (PBS) (*1*), non-labelled ADAPT6-ABD_{035} (*2*), after a single injection of 18 MBq of ^{177}Lu-DOTA-ADAPT6-ABD_{035} (*3*), two injections of 18 MBq of ^{177}Lu-DOTA-ADAPT6-ABD_{035} (*4*) or a single injection of 18 MBq of ^{177}Lu-DOTA-ADAPTNeg-ABD_{035}, which does not bind to HER2 (*5*).[133] Published according to the license https://s100.copyright.com/AppDispatchServlet?publisherName=ELS&contentID=S014296122030627X&-orderBeanReset=true

6.3. Pretargeting

Pretargeting is a two-stage procedure of selective delivery of radionuclides to the tumour.[134] In this case, the targeting molecule is the first to be injected into the body. After it has

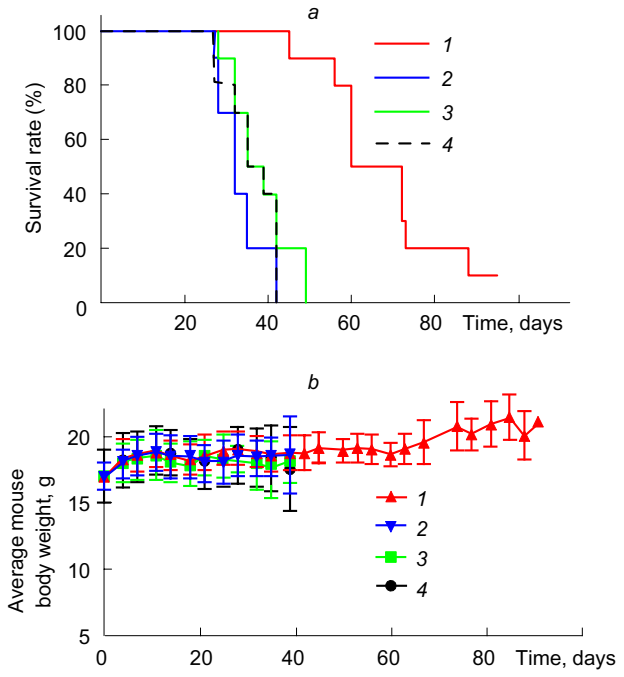


Figure 8. Survival rate of BALB/C nu/nu mice administered with both ZHER2:342-SR-HP1 (ZHP1) targeting agent and labelled ^{177}Lu-HP2 together (*1*), only ^{177}Lu-HP2 (*2*), only ZHER2:342-SR-HP1 (*3*) or PBS (*4*) (*a*), and average mouse body weight during the therapy with the same agents (*b*). [137] Published with permission from publishing company under the license of *Journal of Nuclear Medicine*, Open Access (https://jnm.snmjournals.org/page/permissions).

been localized in the tumour and the excess has been cleared from the blood, tissues and organs, radiolabelled agent capable of specific binding to the targeting molecule is introduced. The labelled agent is usually a relatively small molecule or a short peptide, which rapidly binds to the targeting molecule located in the tumour and is rapidly cleared from blood and intact tissues. This method was developed for the use of the antibodies that reside in the blood for a long time and are rather slowly taken up by tumour cells. In addition, it was proposed to use pretargeting to reduce the radiation damage of kidneys due to the radionuclide therapy involving labelled scaffold proteins.[135, 136] The use of affibodies instead of antibodies has a number of advantages such as fast clearance of the targeting molecule from blood and its slower internalization into tumour cells. Two approaches to the affibody pretargeting were proposed, one being based on bioorthogonal chemistry [135] and the other being based on interaction with peptide nucleic acids (PNA).[136] In both cases, the uptake of the labelled compound in the tumour was more pronounced than that in kidneys. The use of PNA-mediated pretargeting ensured a better ratio between the absorbed doses to the tumour and to kidneys. This therapy considerably increased the survival rate of mice with HER2-expressing xenografts and was not toxic for kidneys (Fig. 8).[137] Further studies showed that the use of PNA nonamer instead of 15-mer additionally reduced the renal uptake of ^{177}Lu and increases twofold the difference between the doses for the tumour and for kidneys.[138]

Owing to modular structure, this system can be easily adapted to other scaffold proteins, *e.g.*, ADAPT and DARPin.

6.4. Effect of the labelling chemistry on the biodistribution of scaffold proteins and their imaging properties

The biodistribution of radioactivity after injection of monoclonal antibodies depends, first of all, on the antigen expression in normal tissues, stability of the label and the degree to which the label can be retained.[139–141] An excessive modification of the antibody *via* conjugation of a superfluous amount of a chelator may have an adverse effect on the label biodistribution,[142] but conjugation of 2–4 chelators per protein molecule is safe and reproducible for different antibodies.[143] Conversely, the chemical nature of the label can considerably affect the biodistribution of short peptides (8–12 amino acids).[57, 144, 145] This effect is quite understandable, since the introduction of a chelator induces noticeable changes in the charge localization and lipophilicity of the peptide. Scaffold proteins have a 5–10 times bigger size than short peptides, and it is not always clear *a priori* whether the labelling strategy would affect their biodistribution, which may be fairly important.

A pronounced influence of the label on the retention of radioactivity in kidneys was observed for ADAPT6.[146] In this study, the scaffold protein was labelled by residualizing (^{111}In) and non-residualizing (^{125}I) radionuclides on the C- or N-ends of the protein (Fig. 9). Four hours after the injection, the renal uptake of the radionuclide was $284 \pm 21\%$ ID g^{-1} (ID is injected dose) for ^{111}In-DOTA-Cys^{59}-ADAPT6, but only $1.7 \pm 0.3\%$ ID g^{-1} for ^{125}I-HPEM-Cys^{59}-ADAPT6. Meanwhile the tumour uptake of the radionuclide was $15 \pm 2\%$ ID g^{-1} for ^{111}In and $22 \pm 3\%$ ID g^{-1} for ^{125}I.

An even more pronounced effect of the label on the biodistribution was noted for the genetically engineered scaffold protein DARPin 9_29 containing 5 ankyrin repeats.[115] In this study, anti-HER2 DARPin 9_29 was labelled either by direct iodination (non-residualizing label) or with ^{99m}Tc(CO)$_3$ using N-terminal hexahistidine tag as the chelator (residualizing label). The use of technetium-99m isotope resulted in a high uptake of the radiopharmaceutical not only in kidneys ($80 \pm 11\%$ ID g^{-1} after 6 h), but also in liver ($27 \pm 4\%$ ID g^{-1} after 6 h) (Fig. 10). Low retention of the radioactive iodine label resulted in its low uptake in kidney ($3.4 \pm 0.4\%$ ID g^{-1}) and liver ($1.2 \pm 0.2\%$ ID g^{-1}) cells at the same time point. The tumour uptake was $3.4 \pm 0.7\%$ ID g^{-1} for radioactive iodine and 2.9 ± 0.7 ID g^{-1} for ^{99m}Tc. A similar beneficial effect was also observed for the DARPin G3 protein containing four ankyrin repeats.[116] Thus, the use of the non-residualizing label reduces the undesirable accumulation of the pharmaceutical in normal tissues without affecting the radionuclide retention in the tumours.

It is noteworthy that a common feature of non-residualizing labels is weak intracellular retention of radioactive metabolites. However, these labels may have considerably different redistribution profiles of these metabolites and effects on the distribution of the labelled protein, and their intracellular retention can also be different. Non-residualizing labels that are formed *via* so-called direct radioiodination are used most often. During the direct radioiodination, the radioactive iodine oxidized *in situ* attacks the hydroxy-

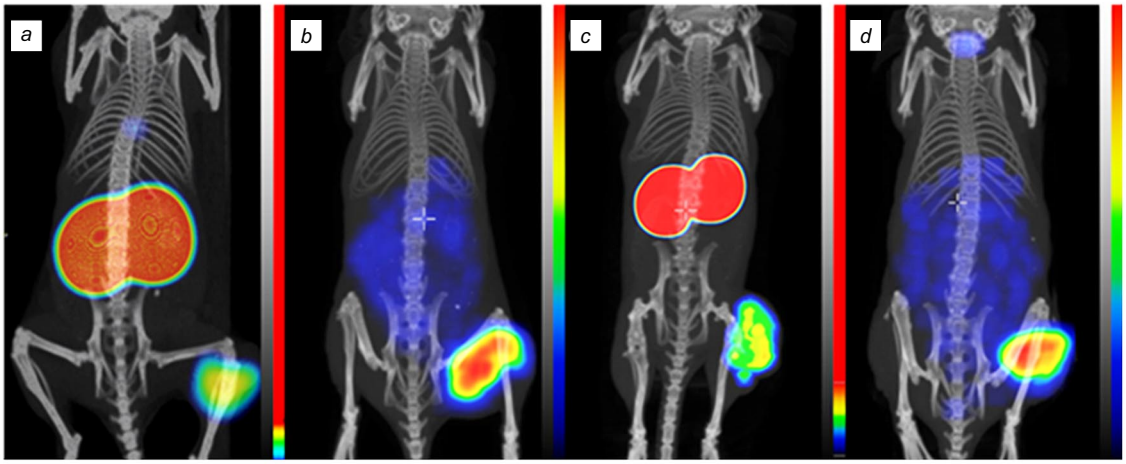


Figure 9. SPECT/CT images (maximum intensity projections) of HER2-expressing xenografts using the ADAPT6 molecule 4 h after the injection (*a* and *c*) of ^{111}In-DOTA-Cys^{2}-ADAPT6 and ^{111}In-DOTA-Cys^{59}-ADAPT6; (*b* and *d*) of ^{125}I-HPEM-Cys^{2}-ADAPT6 and ^{125}I-HPEM-Cys^{59}-ADAPT6.[146] The full linear colour scale adjusted to provide clear imaging of tumours was applied. Published with permission from publishing company under the license of *Journal of Nuclear Medicine*, Open Access (https://jnm.snmjournals.org/page/permissions).

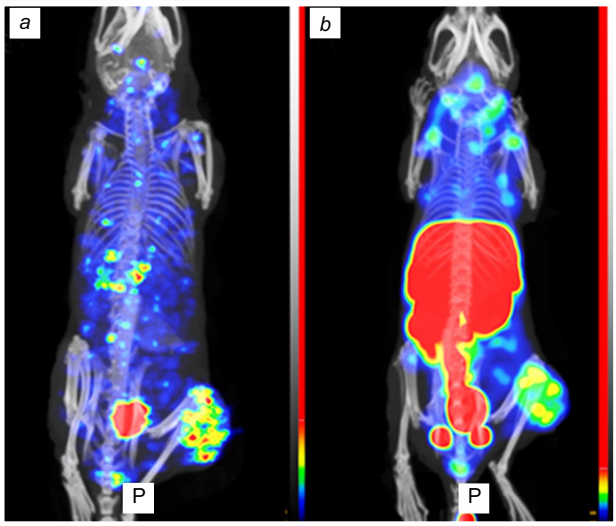


Figure 10. SPECT/CT imaging (maximum intensity projections) of HER2 expression in SKOV-3 xenografts with ^{125}I-DARPin 9_29 (*a*) and ^{99m}Tc(CO)$_3$-DARPin 9_29 (*b*) in small animals 6 h after injection.[115] Published with permission from publishing company under the license https://creativecommons.org/licenses/by/4.0/

phenyl moiety of tyrosine to form a covalent bond. The products of catabolism of directly radioiodinated proteins are radioactive iodotyrosine and iodide. These radiometabolites are accumulated in the thyroid gland, salivary gland and stomach, *i.e.*, in tissues expressing the Na/I symporter (see, for example, Ref. 117). The problem of redistribution of radiometabolites can be solved by using indirect radioiodination of proteins. In this case, small bifunctional molecules are used, containing a functional moiety for radioiodination and a moiety for binding to a functional group of amino acid side chains, usually amino groups of lysine residues or thiol groups of cysteine residues. The reagents suitable for indirect radioiodination of scaffold proteins include *N*-succinimidyl *p*-(trimethylstannyl)benzoate,[87, 147, 148] [2-(4-hydroxyphenyl)ethyl}maleimide (HPEM)[109, 146, 149] and *N*-[4-(tri-n-butylstannylphenethylamino)phenethyl]maleimide.[150] Fragments of the labels that were obtained using these precursors are shown in Fig. 11.

The key drawback of using *N*-succinimidyl *p*-(trimethylstannyl)benzoate is that it binds to the amino group. Since the scaffold protein contains several lysine residues, it is impossible to identify the exact position of the label, and the labelled product is a mixture of proteins labelled in different positions. The conjugation using HPEM and *N*-[4-(tri-n-butylstannylphenethylamino)phenethyl]maleimide results in site-specific labelling. The ADAPT, affibody and DARPin scaffolds do not contain cysteine residues. For this reason, the introduction of the only cysteine residue into the polypeptide using gene engineering methods gives rise to a unique thiol group, and using maleimide it is possible to direct the label exactly to this group. This gives rise to a radiolabelled conjugate with a specified structure. The use of I-HPEM for affibody labelling led to faster clearance of the radionuclide from kidneys in comparison with PIB, although the liver uptake of the pharmaceutical was higher in this case.[109] The affibody labelling with I-PEM provided an even faster decrease in the radioactivity from kidneys than the use of I-HPEM.[150] These data indicate that both the position and the lipophilicity of the radioactive pros-

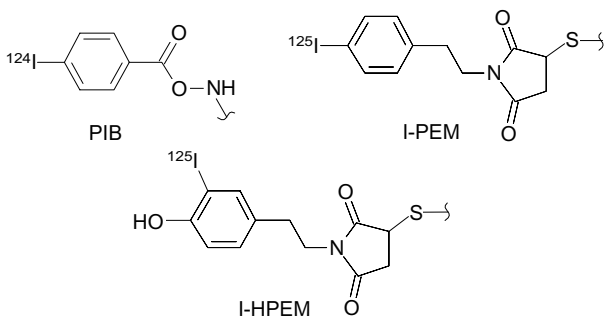


Figure 11. Fragments of the structures of non-residualizing radioactive iodine labels obtained by affibody labelling with PIB, *I-PEM and *I-HPEM.

thetic group affect the elimination of non-residualizing labels from kidneys. It is noteworthy that the use of both labels (I-HPEM and I-PEM) for affibody molecules is accompanied by a marked hepatobiliary excretion and undesired accumulation of the radionuclide in the gastrointestinal tract. It is of interest that the level of hepatobiliary excretion depends on the scaffold structure. When ADAPT was labelled with ^{125}I-HPEM, the level of hepatobiliary excretion was relatively low.[146] In the case of DARPin, the level of hepatobiliary excretion of DARPin G3 labelled with ^{125}I-IPEM was very high,[149] whereas for labelling with ^{125}I-PIB derivative, it was quite acceptable.[148] Thus, there is no universal rule for choosing a non-residualizing label for all scaffold proteins, and the optimal label should be selected experimentally.

Histidine-containing tags are often used to purify recombinant produced proteins by immobilized metal affinity chromatography with immobilized metal. Waibel *et al.*[151] found that the hexahistidine tag can be used as a chelator to label these proteins with $[^{99m}Tc(CO)_3]^+$ (Fig. 12). This approach was successfully utilized to label several targeting proteins.[110, 152, 153] However, the application of hexahistidine tags for labelling the first generation of affibody molecules resulted in an extremely high accumulation of radioactivity in the liver.[154] According to earlier studies, an increase in the hydrophilicity of peptide-based chelators on the N-terminus of affibody molecules reduces the uptake of the label by liver cells, owing to the inclusion of amino acids with negatively charged side chains.[155] Therefore, every other histidine residue in the tag was replaced by a glutamate residue; this gave the HEHEHE, or $(HE)_3$ tag. The *in vivo* experiments demonstrated that the use of the $(HE)_3$ tag, instead of the hexahistidine tag, in the anti-HER2-affibody decreased the liver uptake more than 10-fold.[156] The subsequent studies confirmed that the negative charge of the glutamate is important, since replacement of the glutamate residue with the lysine residue equivalent in the hydrophilic properties, but positively charged only increases the liver uptake of the radionuclide.[157] It is worth noting that in the case of ADAPT6, the replacement of the H_6 tag by $(HE)_3$ led only to a minor decrease in the liver uptake of the radiopharmaceutical,[106] and the replacement of hexahistidine residue in DARPin G3 by the $(HE)_3$ tag also reduced the radionuclide accumulation in liver cells, but only by a factor of three.[158]

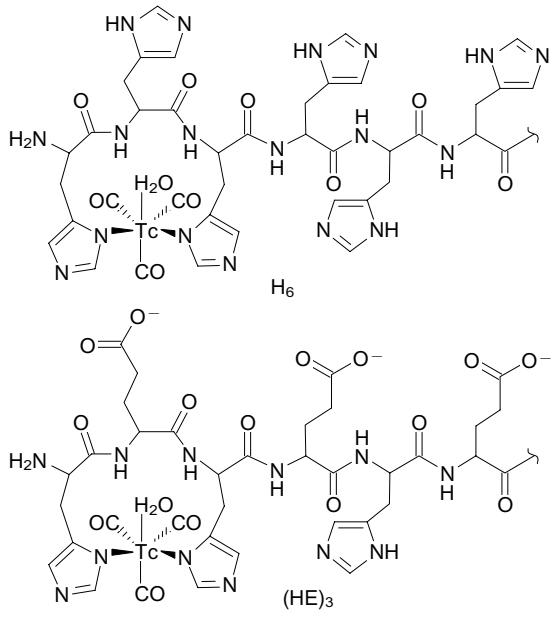


Figure 12. Fragments of the structures of H_6 and $(HE)_3$ tags chelating the $[^{99m}Tc(CO)_3]^+$ cation.

Noteworthy is a publication by Deyev *et al.*,[117] who studied the effect of the chemistry of labelling on the distribution of DARPin Ec1, which binds to EpCAM. Since earlier works addressed DARPin proteins binding to HER2, the authors were going to verify whether the principles established for anti-HER2 DARPin are applicable to DARPin proteins specific to other targets. Direct radioiodination, indirect iodination and $[^{99m}Tc(CO)_3]^+$ labelling using H_6 and $(HE)_3$ tags were tested. The results of the study confirmed the conclusions made for anti-HER2 DARPin (Fig. 13). The tumour uptake of the radionuclide did not change noticeably for different types of labels, while the differences for the normal tissues were pronounced. In the case of $^{99m}Tc(CO)_3$-H_6-Ec1, the uptakes in kidneys, liver and spleen were the highest. The use of $(HE)_3$ for the labelling considerably reduced the uptake in most tissues. Nevertheless, accumulation of $^{99m}Tc(CO)_3$-$(HE)_3$-Ec1 in the liver was higher than that in the tumour. The direct radioiodine label led to a very pronounced decrease in the kidney and liver retention of the radionuclide, but redistribution of radiometabolites gave rise to a higher activity of ^{125}I-H_6-Ec1 in blood and to a higher uptake in the salivary gland and in the stomach. Indirect radioiodination demonstrated the lowest level of radioactivity retention in all organs, except for liver. Thus, the tumour/organs distribution ratios were much higher for ^{125}I-PIB-H_6-Ec1 than for other variants. It is clear that this increases the contrast of imaging and, consequently, the sensitivity of EpCAM molecular detection. This study has clearly demonstrated that selection of the best chemical reagent for labelling is an essential component of the optimal molecular design of targeted drugs based on scaffold proteins.

7. Targeted radionanobioconjugates

Lately, quite a number of chemically diverse nanoparticles (NPs) have been prepared and the interest in the medical applications of hybrid structures based on them has markedly increased. This is due to the unique properties of nanoparticles, which include the physical and chemical stability. Furthermore, NPs have a large surface area, which implies the possibility of attaching functional modules such as therapeutic compounds and biomolecules that recognize the tumour cell receptors and ensure active delivery of the constructs to neoplastic foci.[159–164]

Radionuclides can be either directly encapsulated into nanoparticles or attached to their surface by means of chelators. The key aspects of labelling of various nanoparticles with radioactive isotopes are addressed in reviews,[165, 166] which also give classification of nanoparticles in terms of the technique of their application for the theranostics of neoplastic and other diseases. It turned out that the application of such nanostructures can become an efficient diagnostic method for imaging in nuclear medicine, which would allow the quantitative monitoring of drug delivery and reduce the problems of under- or overdose of the drug. To get acquainted with this issue in more detail, refer to the above publications. Here, we give only a few

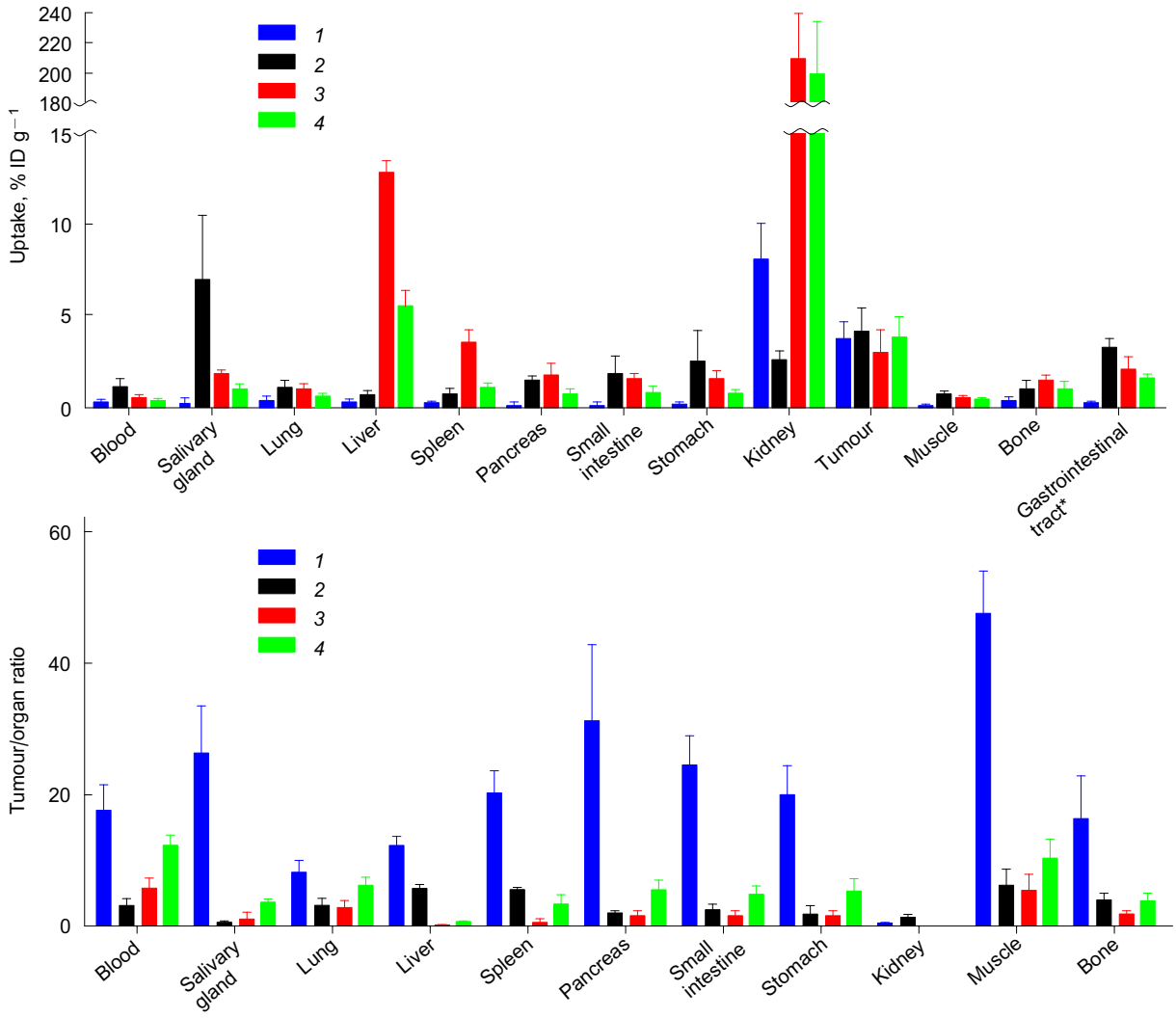


Figure 13. Biodistribution (*a*) and tumour/organ ratios (*b*) for ^{125}I-PIB-H$_6$-Ec1 (*1*), ^{125}I-H$_6$-Ec1 (*2*), ^{99m}Tc(CO)$_3$-H$_6$-Ec1 (*3*) and ^{99m}Tc(CO)$_3$-(HE)$_3$-Ec1 (*4*) in BALB/C nu/nu mice bearing BxPC-3 xenografts 3 h after the injection. The data are presented as mean ± standard deviation for four mice; data for the gastrointestinal tract with content are given as % ID per whole sample.[117] Published with permission from publishing company under the license https://s100.copyright.com/AppDispatchServlet?publisherName=ELS&contentID=S0141813019393808&orderBeanReset=true

examples of various nanomaterials with radioactive labels reported in recent years. Particular attention is given to our own views on the specific benefits and drawbacks of this class of compounds, which are important for evaluating the prospects of their practical use.

Effective radiotherapy of melanomas was shown using ultrasmall (~6 nm) fluorescent silicon nanoparticles bearing the ^{177}Lu beta-emitter and functionalized with a cyclic peptide analogue of alpha-melanocyte stimulating hormone (αMSH). The latter specifically binds to the melanocortin receptor 1 (MC1R) overexpressed on the surface of human melanoma cells.[167]

Mesoporous silicon nanoparticles (~150 nm) functionalized with transferrin, which promoted their accumulation in tumour cells, were used for the targeted delivery of alpha-emitting ^{225}Ac to breast tumours. They showed a good cytotoxic effect accompanied by improved excretion and minimum accumulation of this radioisotope in the bones.[168]

Targeted alpha-therapy with ^{223}Ra and barium ferrite nanoparticles (BaFe-NP) was reported. The radiocytotoxicity of the agents against human ovarian adenocarcinoma (SKOV-3) cells overexpressing HER2 receptor was studied. The radioactive labelling of BaFe nanoparticles was accomplished by replacing Ba cations with ^{223}Ra, and then the nanoparticles were functionalized by covalent conjugation with the antibody trastuzumab (Herceptin®), which provided for high-precision interaction with the HER2 receptor. The hydrodynamic diameter of the NP–trastuzumab conjugate was ~220 nm. The [^{223}Ra]–BaFe–trastuzumab radiobioconjugate strongly held ^{223}Ra (>98%) for 30 days and showed high cytotoxicity against human ovarian adenocarcinoma cells. Owing to its magnetic properties, this conjugate is suitable for drug delivery under the action of a magnetic field.[169] These studies indicate that the multifunctional nanoparticles bearing alpha-emitters are promising for targeted alpha-radiotherapy of various tumours.

Often, tumour cells have more than one, *e.g.*, two or more, cancer specific receptors on the surface. There are known cases in which the resistance to HER2-directed therapy of breast cancer was due to overexpression of

another receptor, particularly epidermal growth factor receptor (EGFR). Yook *et al.*[170] described the development of radiobioconjugates based on 15 nm gold nanoparticles (Au-NPs) for the topical intratumour treatment of breast cancer with radiopharmaceutical targeting both receptors. Gold nanoparticles were modified with polyethylene glycol linked to DOTA chelators to form a complex with beta-emitting ^{177}Lu and conjugated with trastuzumab or panitumumab for targeting HER2 or EGFR, respectively. The study was carried out using tumour cell lines with different levels of expression of these receptors. As was to be expected, radiobioconjugates targeted with antibodies proved to be more cytotoxic for tumour cells than non-targeted ^{177}Lu-Au-NPs. Also, what is more important, combination of two targeted radiobioconjugates was in all cases markedly more efficient for the destruction of breast cancer cells that simultaneously expressed HER2 and EGFR than the separate use of targeted ^{177}Lu and Au-NPs.

During the therapy, tumour cells can change, which gives rise to drug resistance and recurrent and metastatic cancer. A promising approach for overcoming these problems is combined therapy, which means the use of compounds with different mechanisms of action (radio-, immuno- and chemotherapy).[4, 171–174]

Modern nanotechnologies make it possible to fabricate multifunctional structures containing simultaneously several toxic agents. Nanoparticles based on polyethyleneimine with hyaluronic acid, which efficiently binds to glycoprotein CD44, overexpressed in various solid tumours, and thus promotes targeted drug delivery, were fabricated for the targeted combined therapy of the anaplastic thyroid carcinoma.[175] These particles had tyrosine residues, which can be radiolabelled with $^{131/125}$I, and contained a low-molecular-weight therapeutic agent PRIMA-1 for reactivation of p53 tumour suppressor protein *via* its reduction. The combined delivery of these two agents induced an impressive anti-tumour effects owing to radiosensitization of PRIMA-1 by the beta-radiation of ^{131}I.

Guryev *et al.*[176] described upconversion nanoparticles (UCNP, hydrodynamic diameter of ~90 nm) $NaYF_4$:Yb,Tm/$NaYF_4$ in which some of yttrium atoms were replaced by beta-emitting ^{90}Y, and a fragment of the exotoxin A from *Pseudomonas aeruginosa* (PE40) with HER2 -specific DARPin 9_29 peptide was attached to the surface of nanomaterial (Fig. 14).

An important characteristic of upconversion nanoparticles is the ability to convert near-IR light, which deeply penetrates into biological tissues, into visible and UV radiation. Upon systemic administration to mice with grafted HER2-positive human tumours, these nanostructures efficiently accumulated in the tumours; this allowed obtaining high-contrast images and hence demonstrated the possibility of non-invasive fluorescent detection of malignant neoplasms. Testing of the therapeutic potential of these multifunctional complexes demonstrated that combined delivery of two toxic agents, ^{90}Y and PE40, brings about a considerable synergistic action: the same effect on tumour cells was observed at ~2200 times lower concentrations than in the case of separate use of these agents.

This study illustrates an important benefit of nanoparticles, namely, the possibility of fabrication of nanoparticle-based hybrid multimodal structures for cancer theranostics. One more benefit provided by the use of most nanostructures is the absence of significant undesirable accumulation in kidneys. This is due to the fact that

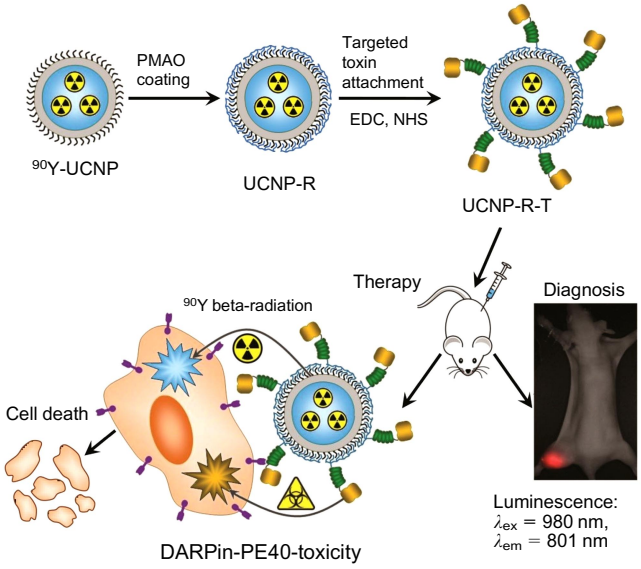


Figure 14. Assembly and mechanism of action of the hybrid multifunctional nanocomplex UCNP-R-T. UCNP are up-conversion nanoparticles; R is ^{90}Y radionuclide; T is fragment of exotoxin A from *Pseudomonas aeruginosa* (PE40) connected to the targeting peptide (DARPin 9_29); PMAO is amphiphilic alternating copolymer of maleic anhydride and 1-octadecene; EDC is *N*-(3-dimethylaminopropyl)-*N*′-ethylcarbodiimide hydrochloride; NHS is *N*-hydroxysulfosuccinimide sodium salt.[176] Published with permission from publishing company under the license https://www.pnas.org/page/about/rights-permissions

glomerular filtration passes through pores with an average diameter of 2.9 nm. With this size of pores, virtually all nanoparticles, especially negatively charged nanoparticles equipped with targeting peptides, are retained in the blood plasma and do not get into the primary urine.

Meanwhile, the physicochemical properties of most nanoparticles, primarily their size, are also responsible for their two main drawbacks. The first one is related to fast clearance of these agents from blood stream by the cells of mononuclear phagocyte system and the complement system, which results in high liver and spleen uptakes of the particles and has an adverse effect on the efficiency of their delivery to the tumour. The second one is that, despite the enhanced penetrability of the tumour vessels and the retention effect characteristic of many tumours, bulky nanostructures poorly penetrate into tumours and the amount of the drug delivered in this way is not always sufficient.

The former problem of too fast elimination of nanoparticles from blood has been traditionally tackled by coating nanoparticles by inert polymers that hide them from the physiological protection systems of the body.[177] Most often, this was done using stealth polymers such as polyethylene glycol, poly(2-oxazoline) and poly(zwitter ions). To date, clinical success has been achieved for stealth liposomes surface-modified with inert polymers that hide them from the immune system. Attempts were also made to optimize the tumour uptake of nanoparticles by changing the shape, surface area and size of nanostructures. Comparison of the action of 50 nm gold nanoparticles shaped like nanospheres, nanoplates or nanorings showed that the last-mentioned shape ensured the lowest absorption by mononuclear phagocytes and the highest accumulation in the tumour.[178]

However, it should be admitted that generally the problem of poor pharmacokinetics of nanoparticles has not yet been solved. Nikitin *et al.*[179] proposed a new approach that considerably (up to 32-fold) increased the time of blood circulation of nanoagents and, as a consequence, enhanced their therapeutic efficiency. This technique, called mononuclear phagocyte system cytoblockade, includes the injection of allogenic anti-erythrocyte antibodies. As a result, by analogy of the natural process where the immune system continuously eliminates spent red blood cells from the circulation, the immune system concentrates on the attack on the own red blood cells and for several hours it cannot see the injected nanostructures. During this period, the nanostructures can find the target neoplastic growth, deliver the drug and ensure the therapeutic action. In addition, the decrease in hematocrit ($\sim$5%) was temporary, and the depletion of red blood cells in experimental animals did not cause significant physiological disorders. This technique is universal, because it does not require modification of the nanoparticles themselves.

The increase in the circulation time of therapeutic nanoparticles by blocking the mononuclear phagocyte system can also be attained in another way: preliminary injection of non-functional non-stealth nanoagents that draw an attack of the immune system to themselves.[180–182]

In order to select such agents, factors affecting the blood circulation of blocking nanoparticles, such as size, charge, type of coating and frequency of injection, were studied. Compounds that block the mononuclear phagocyte system and thus prolong the blood half-life of functional particles by factors of up to 18 were proposed. Unlike the technique described above, the application of blocking non-stealth nanoagents does not induce a decrease in the hematocrit. These studies demonstrate potential methods that can prolong the blood half-life of nanoagents, which improves the delivery of diagnostic and therapeutic compounds into tumours and results in their mild effect on critically important organs, *i.e.*, the liver and spleen.

The second problem associated with the use of nanomaterials is caused by their hindered penetration into solid tumours. Carcinomas have tight intercellular junctions that maintain the integrity of solid epithelial tumours and prevent the penetration of bulky anticancer drugs such as full-length antibodies deep into the tumour. In the areas of intercellular junctions of epithelial cells, functioning of the desmoglein 2 protein ensures the structural adhesion of neighbouring cells. A small recombinant protein called junction opener (JO) was developed; it binds desmoglein 2, thus causing temporary and specific opening of tight junctions, which allows various therapeutic agents to penetrate into tumours.[183–187]

The combined introduction of JO and monoclonal antibodies or chemotherapeutic agents markedly increases their efficiency, because it provides for the enhanced drug penetration into the tumour. Wang *et al.*[188] studied the potential of JO as applied to nanomaterials of different size in relation to pegylated gold nanoparticles. It was shown that JO markedly increases the tumour accumulation of nanoparticles with a size of 35 nm, but not 120 nm. Thus, junction opener is a promising agent; when used in combination with targeted nanomaterials, it can promote their efficient accumulation both around and inside the tumour. This is especially significant for inoperable cancer.[189] It is of interest whether it is possible to simultaneously minimize both drawbacks of nanomaterials indicated above (accumulation in the liver and poor penetration into the tumour) by combining the technique of blocking the mononuclear phagocyte system and use of junction opener. In the case of success, this could give rise to a new strategy of cancer theranostics. Additional benefits may be provided by systems that use intracellular transport pathways to deliver radionuclides into malignant cell nuclei.[190, 191]

8. Conclusion

The success of modern oncology is closely related to the active use of targeted pharmaceutical drugs. Their action is based on specific recognition of molecular anomalies inherent in malignant neoplasms, which are expressed in tumour cells and stromal tumour components. Today, monoclonal antibodies constitute the main class of modern targeted antitumour therapeutic agents. The main drawbacks of full-length antibodies is their large size, which accounts for slow clearance, extravasation and unsatisfactory penetration into the tumour.

Targeting molecules are used to transport toxins, drugs or cytotoxic radionuclides to tumour cells. The targeted delivery of radionuclides helps to solve significant problems of cancer therapy, including personalization of medicine and overcoming multiple drug resistance.

Currently, only two vectors have shown their obvious clinical efficacy for targeted radionuclide therapy of malignant tumours, particularly, somatostatin analogues and prostate-specific membrane antigen inhibitors, which are small-size peptides. The success of using these agents indicates that a decrease in the size of targeted molecules is a promising strategy for the development of new therapeutic radiopharmaceuticals.

Therefore, a topical issue is bioengineering of small-sized targeting molecules. High-affinity ligands can be based on robust scaffolds consisting of amino acids. A considerable advantage of scaffold proteins over antibodies is their smaller size; these molecules are obtained by chemical synthesis or by low-cost bacterial production, which makes them markedly cheaper compared to antibodies. One more advantage of these compounds is that they are able to restore their properties and high affinity to molecular targets after the thermal or chemical denaturation.

The chemistry of labelling markedly affects the pharmacokinetic properties of protein radiopharmaceuticals. Studies in this area are directed towards both improving the targeting properties of the compounds and decrease in their accumulation in non-target organs and tissues.

One of the promising approaches to solving this problem is pretargeting, which represents a two-stage procedure of selective delivery of radionuclides to the tumour. In this case, the targeting molecule is the first to be injected into the body and, after this molecule has been localized in the tumour and the excess has been eliminated from blood, tissues and organs, the radiolabelled agent capable of specific binding to the targeting molecule is introduced into the body. The labelled compound is usually a relatively small molecule or short peptide, which rapidly binds to the targeting agent located in the tumour and is rapidly eliminated from blood and intact tissues.

The use of targeted nanoparticles may become a potent tool of cancer theranostics provided that the problems of their capture by the mononuclear phagocyte system and

accumulation in the tumour have been solved. This can be done by blocking of the mononuclear phagocyte system by preliminary injection of allogenic anti-erythrocyte antibodies or non-functional non-stealth nanoagents, which draw the attack by the immune system to themselves. These blocking would make it possible to prolong the circulation time of nanoagents in the blood and, as a result, increase their therapeutic activity.

The reported study was funded by RFBR, Project Nos 20-14-50055 and 19-54-06001.

9. List of acronyms

The following acronyms are used in the review

ABD — albumin-binding domain,

ADAPT — peptide based on albumin-binding domain of 46 amino acids of the streptococcus protein G,

Affibody — scaffold protein based on the Z-domain of protein A,

CDTPA — cyclic anhydride of diethylenetriaminepentaacetic acid,

CT — computed tomography,

DARPin — design ankyrin repeat protein,

DFO — desferrioxamine (Desferral®),

DOTA — 1,4,7,10-tetraazacyclododecane-1,4,7,10-tetraacetic acid,

DOTATATE — D-Phe-Cys-Phe-D-Trp-Lys-Thr-Cys-The octapeptide covalently bound to the DOTA chelator,

DOTATOC — (DOTA^0-Phe^1-Tyr^3)-octreotide,

DTPA — diethylenetriaminepentaacetate,

EpCAM — epithelial cell adhesion molecule, a membrane protein,

HER1 (EGFR) — human epidermal growth factor receptor type 1,

HER2 — human epidermal growth factor receptor type 2,

HPEM — [2-(4-hydroxyphenyl)ethyl]maleimide,

ID — injected dose,

I-PEM — [2-(4-iodophenyl)ethyl]maleimide,

I-PIB — *p*-iodobenzoate,

NP — nanoparticle,

PBS — phosphate buffered saline,

PET — positron emission tomography,

PNA — peptide nucleic acid,

PSMA — prostate-specific membrane antigen,

SPECT — single-photon emission computed tomography.

10. References

1. B.G.Smaglo, D.Aldeghaither, L.M.Weiner. *Nat. Rev. Clin. Oncol.*, **11**, 637 (2014)
2. R.Mazor, M.Onda, I.Pastan. *Immunol. Rev.*,**270**, 152 (2016)
3. A.V.Stepanov, A.A.Belogurov Jr., N.A.Ponomarenko, O.A.Stremovskiy, L.V.Kozlov, A.M.Bichucher, S.E.Dmitriev, I.V.Smirnov, O.G.Shamborant, D.S.Balabashin, L.P.Sashchenko, A.G.Tonevitsky, A.Friboulet, A.G.Gabibov, S.M.Deyev. *PLoS One*, **6**, e20991 (2011)
4. E.Shramova, G.Proshkina, V.Shipunova, A.Ryabova, R.Kamyshinsky, A.Konevega, A.Schulga, E.Konovalova, G.Telegin, S.Deyev. *Cancers (Basel)*, **12**, 3014 (2020)
5. S.Verma, D.Miles, L.Gianni, I.E.Krop, M.Welslau, J.Baselga, M.Pegram, D.Y.Oh, V.Diäras, E.Guardino, L.Fang, M.W.Lu, S.Olsen, K.Blackwell. *New Eng. J. Med.*, **367**, 1783 (2012)
6. S.J.Keam. *Drugs*, **80**, 501 (2020)
7. S.M.Larson, J.A.Carrasquillo, N.K.Cheung, O.W.Press. *Nat. Rev. Cancer*, **15**, 347 (2015)
8. *Natsional'noe Rukovodstvo po Radionukleidnoi Diagnostike. (National Guidelines for Radionuclide Diagnostics)*. (Eds Yu.B.Lishmanov, V.I.Chernov). (Tomsk: STT, 2010)
9. S.H.Giordano, S.Temin, J.J.Kirshner, S.Chandarlapaty, J.R.Crews, N.E.Davidson, F.J.Esteva, A.M.Gonzalez-Angulo, I.Krop, J.Levinson, N.U.Lin, S.Modi, D.A.Patt, E.A.Perez, J.Perlmutter, N.Ramakrishna, E.P.Winer. *J. Clin. Oncol.*, **32**, 2078 (2014)
10. E.Van Cutsem, Y.J.Bang, F.Feng-Yi, J.M.Xu, K.W.Lee, S.C.Jiao, J.L.Chong, R.I.López-Sanchez, T.Price, O.Gladkov, O.Stoss, J.Hill, V.Ng, M.Lehle, M.Thomas, A.Kiermaier, J.Rüschoff. *Gastric Cancer*, **18**, 476 (2015)
11. Y.J.Bang, E.Van Cutsem, A.Feyereislova, H.C.Chung, L.Shen, A.Sawaki, F.Lordick, A.Ohtsu, Y.Omuro, T.Satoh, G.Aprile, E.Kulikov, J.Hill, M.Lehle, J.Rüschoff, Y.-K.Kang. *Lancet*, **376**, 687 (2010)
12. L.Gianni, T.Pienkowski, Y.H.Im, L.Roman, L.M.Tseng, M.C.Liu, A.Lluch, E.Staroslawska, J.de la Haba-Rodriguez, S.A.Im, J.L.Pedrini, B.Poirier, P.Morandi, V.Semiglazov, V.Srimuninnimit, G.Bianchi, T.Szado, J.Ratnayake, G.Ross, P.Valagussa. *Lancet Oncol.*, **13**, 25 (2012)
13. E.de Azambuja, A.P.Holmes, M.Piccart-Gebhart, E.Holmes, S.Di Cosimo, R.F.Swaby, M.Untch, C.Jackisch, I.Lang, I.Smith, F.Boyle, B.Xu, C.H.Barrios, E.A.Perez, H.A.Azim Jr, S.-B.Kim, S.Kuemmel, C.-S.Huang, P.Vuylsteke, R.-K.Hsieh, V.Gorbunova, A.Eniu, L.Dreosti, N.Tavartkiladze, R.D.Gelber, H.Eidtmann, J.Baselga. *Lancet Oncol.*, **15**, 1137 (2014)
14. D.J.Slamon, G.M.Clark, S.G.Wong, W.J.Levin, A.Ullrich, W.L.McGuire. *Science*, **235**, 177 (1987)
15. T.Foukakis, G.Åström, L.Lindström, T.Hatschek, J.Bergh. *Ann. Oncol.*, **23**, x349 (2012)
16. N.Houssami, P.Macaskill, R.L.Balleine, M.Bilous, M.D.Pegram. *Breast Cancer Res. Treat.*, **129**, 659 (2011)
17. U.Wilking, E.Karlsson, L.Skoog, T.Hatschek, E.Lidbrink, G.Elmberger, H.Johansson, L.Lindström, J.Bergh. *Breast Cancer Res. Treat.*, **125**, 553 (2011)
18. V.Tolmachev, S.Stone-Elander, A.Orlova. *Lancet Oncol.*, **11**, 992 (2010)
19. V.Tolmachev, A.Orlova. *Cancers (Basel)*, **12**, 651 (2020)
20. V.Garousi, A.Orlova, F.Y.Frejd, V.Tolmachev. *EJNMMI Radiopharm. Chem.*, **5**, 16 (2020)
21. A.Krasniqi, M.D'Huyvetter, N.Devoogdt, F.Y.Frejd, J.Sörensen, A.Orlova, M.Keyaerts, V.Tolmachev. *J. Nucl. Med.*, **59**, 885 (2018)
22. P.W.Miller, N.J.Long, R.Vilar, A.D.Gee. *Angew. Chem., Int. Ed.*, **47**, 8998 (2008)
23. G.A.van Dongen, G.W.Visser, M.N.Lub-de Hooge, E.G.de Vries, L.R. Perk. *Oncologist*, **12**, 1379 (2007)
24. V.Tolmachev, S.Stone-Elander. *Biochim. Biophys. Acta*, **1800**, 487 (2010)
25. L.E.Lamberts, S.P.Williams, A.G.Terwisscha van Scheltinga, M.N.Lub-de Hooge, C.P.Schröder, J.A.Gietema, A.H.Brouwers, E.G.de Vries. *J. Clin. Oncol.*, **33**, 1491 (2015)
26. G.A.M.S.van Dongen, W.Beaino, A.D.Windhorst, G.J.C.Zwezerijnen, D.E.Oprea-Lager, N.H.Hendrikse, C.van Kuijk, R.Boellaard, M.C.Huisman, D.J.Vugts. *J. Nucl. Med.*, **62**, 438 (2021)
27. B.D.Wright, S.E.Lapi. *J. Nucl. Med.*, **54**, 1171 (2013)
28. W.Wei, Z.T.Rosenkrans, J.Liu, G.Huang, Q.Y.Luo, W.Cai. *Chem. Rev.*, **120**, 3787 (2020)
29. E.C.Dijkers, T.H.Oude Munnink, J.G.Kosterink, A.H.Brouwers, P.L.Jager, J.R.de Jong, G.A.van Dongen, C.P.Schröder, M.N.Lub-de Hooge, E.G.de Vries. *Clin. Pharmacol. Ther.*, **87**, 586 (2010)

30. M.H.Jansen, S.E.M.Veldhuijzen van Zanten, D.G.van Vuurden, M.C.Huisman, D.J.Vugts, O.S.Hoekstra, G.A.van Dongen, G.L.Kaspers. *J. Nucl. Med.*, **58**, 711(2017)
31. I.Verel, G.W.Visser, R.Boellaard, M.Stigter-van Walsum, G.B.Snow, G.A.van Dongen. *J. Nucl. Med.*, **44**, 1271 (2003)
32. E.Dolgin. *Nat. Biotechnol.*, **36**, 1125 (2018)
33. V.Tolmachev. In *Targeted Radionuclide Tumor Theraphy, Biological Aspects*. (Eds T.Stigbrand J.Carlsson, G.P.Adams). (Netherlands: Springer, 2008)
34. R.W.Howell, D.V.Rao, K.S.Sastry. *Med. Phys.*, **16**, 66 (1989)
35. T.E.Wheldon, J.A.O'Donoghue. *Int. J. Radiat. Biol.*, **58**, 1 (1990)
36. T.E.Wheldon, J.A.O'Donoghue, A.Barrett, A.S.Michalowski. *Radiother. Oncol.*, **21**, 91 (1991)
37. J.A.O'Donoghue, M.Bardies, T.E.Wheldon. *J. Nucl. Med.*, **36**, 1902 (1995)
38. J.Zweit. *Phys. Med. Biol.*, **41**, 1905 (1996)
39. S.Srivastava, E.Dadachova. *Semin. Nucl. Med.*, **31**, 330 (2001)
40. *Table of Nuclides — Nuclear Structure and Decay Data*; https://www-nds.iaea.org/relnsd/vcharthtml/VChartHTML.html (last accessed 02.02.2022)
41. J.P.Pouget, I.Navarro-Teulon, M.Bardiès, N.Chouin, G.Cartron, A.Pèlegrin, D.Azria. *Nat. Rev. Clin. Oncol.*, **8**, 720 (2011)
42. R.M.de Kruijff, H.T.Wolterbeek, A.G.Denkova. *Pharmaceuticals (Basel)*, **8**, 321 (2015)
43. V.Tolmachev, J.Carlsson, H.Lundqvist. *Acta Oncol.*, **43**, 264 (2004)
44. V.Tolmachev, A.Orlova, H.Lundqvist. *Curr. Med. Chem.*, **10**, 2447 (2003)
45. D.J.Hnatowich. *Int. J. Rad. Appl. Instrum., B*, **13**, 353 (1986)
46. D.J.Hnatowich, F.Virzi, M.Fogarasi, M.Rusckowski, P.Winnard Jr. *Nucl. Med. Biol.*, **21**, 1035 (1994)
47. B.V.Egorova, O.A.Fedorova, S.N.Kalmykov. *Russ. Chem. Rev.*, **88**, 901 (2019)
48. T.I.Kostelnik, C.Orvig. *Chem. Rev.*, **119**, 902 (2019)
49. R.D.Hancock. *J. Chem. Educ.*, **69**, 615 (1992)
50. G.P.Nicolas, R.Mansi, L.McDougall, J.Kaufmann, H.Bouterfa, D.Wild, M.Fani. *J. Nucl. Med.*, **58**, 1435 (2017)
51. B.Mitran, S.S.Rinne, M.W.Konijnenberg, T.Maina, B.A.Nock, M.Altai, A.Vorobyeva, M.Larhed, V.Tolmachev, M.de Jong, U.Rosenström, A.Orlova. *Int. J. Cancer*, **145**, 3347 (2019)
52. N.M.Grob, D.Häussinger, X.Deupi, R.Schibli, M.Behe, T.L.Mindt. *J. Med. Chem.*, **63**, 4484 (2020)
53. P.M.Smith-Jones, S.Vallabahajosula, S.J.Goldsmith, V.Navarro, C.J.Hunter, D.Bastidas, N.H.Bander. *Cancer Res.*, **60**, 5237 (2000)
54. M.Moreau, O.Raguin, J.M.Vrigneaud, B.Collin, C.Bernhard, X.Tizon, F.Boschetti, O.Duchamp, F.Brunotte, F.Denat. *Bioconjug. Chem.*, **23**, 1181 (2012)
55. D.Lindenblatt, N.Terraneo, G.Pellegrini, S.Cohrs, P.R.Spycher, D.Vukovic, M.Béhé, R.Schibli, J.Grünberg. *BMC Cancer*, **18**, 922 (2018)
56. Y.Maina, R.Cescato, B.Waser, A.Tatsi, A.Kaloudi, E.P.Krenning, M.de Jong, B.A.Nock, J.C.Reubi. *J. Med. Chem.*, **57**, 6564 (2014)
57. A.Heppeler, J.P.André, I.Buschmann, X.Wang, J.C.Reubi, M.Hennig, T.A.Kaden, H.R.Maecke. *Chemistry*, **14**, 3026 (2008)
58. C.A.Umbricht, M.Benesová, R.M.Schmid, A.Türler, R.Schibli, N.P.van der Meulen, C.Müller. *EJNMMI Res.*, **7**, 9 (2017)
59. A.Loktev, T.Lindner, W.Mier, J.Debus, A.Altmann, D.Jäger, F.Giesel, C.Kratochwil, P.Barthe, C.Roumestand, U.Haberkorn. *J. Nucl. Med.*, **59**, 1423 (2018)
60. K.Siwowska, P.Guzik, K.A.Domnanich, J.M.Monné Rodríguez, P.Bernhardt, B.Ponsard, R.Hasler, F.Borgna, R.Schibli, U.Köster, N.P.van der Meulen, C.Müller. *Pharmaceutics*, **11**, 424 (2019)
61. M.Benesová, M.Schäfer, U.Bauder-Wüst, A.Afshar-Oromieh, C.Kratochwil, W.Mier, U.Haberkorn, K.Kopka, M.Eder. *J. Nucl. Med.*, **56**, 914 (2015)
62. H.S.Chan, M.W.Konijnenberg, E.de Blois, S.Koelewijn, R.P.Baum, A.Morgenstern, F.Bruchertseifer, W.A.Breeman, M.de Jong. *EJNMMI Res.*, **6**, 6 (2016)
63. V.Y.Stenberg, A.Juzeniene, Q.Chen, X.Yang, Ø.S.Bruland, R.H.Larsen. *J. Labelled Compd. Radiopharm.*, **63**, 129 (2020)
64. Y.Qin, S.Imobersteg, A.Blanc, S.Frank, R.Schibli, M.P.Béhé, M.Grzmil. *Pharmaceutics*, **12**, 1088 (2020)
65. H.Heyerdahl, N.Abbas, E.M.Brevik, C.Mollatt, J.Dahle. *PLoS One*, **7**, e42345 (2012)
66. M.Hens, G.Vaidyanathan, X.G.Zhao, D.D.Bigner, M.R.Zalutsky. *Nucl. Med. Biol.*, **37**, 741 (2010)
67. D.A.Vallera, M.Elson, M.W.Brechbiel, K.E.Dusenbery, L.J.Burns, K.M.Skubitz, W.B.Jaszcz, N.K.Ramsay, A.Panoskaltsis-Mortari, D.W.Kuroki, J.E.Wagner, J.H.Kersey. *Cancer Biother. Radiopharm.*, **18**, 133 (2003)
68. F.Lansigan, C.A.Costa, B.I.Zaki, S.P.Yen, E.S.Winer, H.Ryan, D.Findley, S.R.Metzler, L.Shaw, B.Toaso, T.A.MacKenzie, Y.Chen, A.W.Beaven. *Clin. Cancer Res.*, **25**, 6073 (2019)
69. M.Iino, Y.Sakamoto, T.Sato. *Hematology*, **24**, 623 (2019)
70. V.Tolmachev, H.Wúllberg, K.Andersson, A.Wennborg, H.Lundqvist, A.Orlova. *Eur. J. Nucl. Med. Mol. Imaging*, **36**, 1460 (2009)
71. M.Persson, V.Tolmachev, K.Andersson, L.Gedda, M.Sandström, J.Carlsson. *Eur. J. Nucl. Med. Mol. Imaging*, **32**, 1457 (2005)
72. F.T.Lee, A.J.Mountain, M.P.Kelly, C.Hall, A.Rigopoulos, T.G.Johns, F.E.Smyth, M.W.Brechbiel, E.C.Nice, A.W.Burgess, A.M.Scott. *Clin. Cancer Res.*, **11**, 7080s (2005)
73. T.K.Nayak, C.A.Regino, K.J.Wong, D.E.Milenic, K.Garmestani, K.E.Baidoo, L.P.Szajek, M.W.Brechbiel. *Eur. J. Nucl. Med. Mol. Imaging*, **37**, 1368 (2010)
74. S.Heskamp, R.Raavé, O.Boerman, M.Rijpkema, V.Goncalves, F.Denat. *Bioconjug. Chem.*, **28**, 2211 (2017)
75. E.C.Dijkers, J.G.Kosterink, A.P.Rademaker, L.R.Perk, G.A.van Dongen, J.Bart, J.R.de Jong, E.G.de Vries, M.N.Lub-de Hooge. *J. Nucl. Med.*, **50**, 974 (2009)
76. D.J.Vugts, C.Klaver, C.Sewing, A.J.Poot, K.Adamzek, V.Huegli, C.Mari, G.W.Visser, I.E.Valverde, G.Gasser, T.L.Mindt, G.A.van Dongen. *Eur. J. Nucl. Med. Mol. Imaging*, **44**, 286 (2017)
77. R.Raavé, G.Sandker, P.Adumeau, C.B.Jacobsen, F.Mangin, M.Meyer, M.Moreau, C.Bernhard, L.Da Costa, A.Dubois, V.Goncalves, M.Gustafsson, M.Rijpkema, O.Boerman, J.C.Chambron, S.Heskamp, F.Denat. *Eur. J. Nucl. Med. Mol. Imaging*, **46**, 1966 (2019)
78. J.Malmberg, V.Tolmachev, A.Orlova. *Int. J. Oncol.*, **38**, 1137 (2011)
79. M.Bourgeois, C.Bailly, M.Frindel, Guerard, M.Chérel, A.Faivre-Chauvet, F.Kraeber-Bodéré, C.Bodet-Milin. *Expert Opin. Biol. Ther.*, **17**, 813 (2017)
80. H.J.Wester, H.Kessler. *J. Nucl. Med.*, **46**, 1940 (2005)
81. J.Kunikowska, L.Królicki, A.Hubalewska-Dydejczyk, R.Mikolajczak, A.Sowa-Staszczak, D.Pawlak. *Eur. J. Nucl. Med. Mol. Imaging*, **38**, 1788 (2011)
82. C.Kratochwil, F.Bruchertseifer, H.Rathke, M.Bronzel, Ch.Apostolidis, W.Weichert, U.Haberkorn, F.L.Giesel, A.Morgenstern. *J. Nucl. Med.*, **58**, 1624 (2017)
83. Sh.Okamoto, A.Thieme, J.Allmann, C.D'Alessandria, T.Maurer, M.Retz, R.Tauber, M.M.Heck, H.-J.Wester, N.Tamaki, W.P.Fendler, K.Herrmann, C.H.Pfob, K.Scheidhauer, M.Schwaiger, S.Ziegler, M.Eiber. *J. Nucl. Med.*, **58**, 445 (2017)
84. K.Rahbar, M.Weckesser, S.Huss, A.Semjonow, H.-J.Breyholz, A.J.Schrader, M.Schäfers, M.Bögemann. *J. Nucl. Med.*, **57**, 563 (2016)
85. C.Jost, A.Plückthun. *Curr. Opin. Struct. Biol.*, **27**, 102 (2014)

86. K.Nord, E.Gunneriusson, J.Ringdahl, S.Ståhl, M.Uhlén, P.A.Nygren. *Nat. Biotechnol.*, **15**, 772 (1997)
87. A.Orlova, M.Magnusson, T.L.Eriksson, M.Nilsson, B.Larsson, I.Höidén-Guthenberg, C.Widström, J.Carlsson, V.Tolmachev, S.Ståhl, F.Y.Nilsson. *Cancer Res.*, **66**, 4339 (2006)
88. H.Wúllberg, A.Orlova, M.Altai, S.J.Hosseinimehr, C.Widström, J.Malmberg, S.Ståhl, V.Tolmachev. *J. Nucl. Med.*, **52**, 461 (2011)
89. M.Friedman, A.Orlova, E.Johansson, T.L.Eriksson, I.Höidén-Guthenberg, V.Tolmachev, F.Y.Nilsson, S.Ståhl. *J. Mol. Biol.*, **376**, 1388 (2008)
90. V.Tolmachev, M.Friedman, M.Sandström, T.L.Eriksson, D.Rosik, M.Hodik, S.Ståhl, F.Y.Frejd, A.Orlova. *J. Nucl. Med.*, **50**, 274 (2009)
91. V.Tolmachev, D.Rosik, H.Wållberg, A.Sjöberg, M.Sandström, M.Hansson, A.Wennborg, A.Orlova. *Eur. J. Nucl. Med. Mol. Imaging*, **37**, 613 (2010)
92. M.Malm, N.Kronqvist, H.Lindberg, L.Gudmundsdotter, T.Bass, F.Y.Frejd, I.Höidén-Guthenberg, Z.Varasteh, A.Orlova, V.Tolmachev, S.Ståhl, J.Löfblom. *PLoS One*, **8**, e62791 (2013)
93. V.Tolmachev, J.Malmberg, C.Hofström, L.Abrahmsén, T.Bergman, A.Sjöberg, M.Sandström, T.Gräslund, A.Orlova. *J. Nucl. Med.*, **53**, 90 (2012)
94. V.Tolmachev, Z.Varasteh, H.Honarvar, S.J.Hosseinimehr, O.Eriksson, P.Jonasson, F.Y.Frejd, L.Abrahmsen, A.Orlova. *J. Nucl. Med.*, **55**, 294 (2014)
95. B.Mitran, R.Güler, F.P.Roche, E.Lindström, R.K.Selvaraju, F.Fleetwood, S.S.Rinne, L.Claesson-Welsh, V.Tolmachev, S.Ståhl, A.Orlova, J.Löfblom. *Theranostics*, **8**, 4462 (2018)
96. D.E.González Trotter, X.Meng, P.McQuade, D.Rubins, M.Klimas, Z.Zeng, B.M.Connolly, P.J.Miller, S.S.O'Malley, S.A.Lin, K.L.Getty, L.Fayadat-Dilman, L.Liang, E.Wahlberg, O.Widmark, C.Ekblad, F.Y.Frejd, E.D.Hostetler, J.L.Evelhoch. *J. Nucl. Med.*, **58**, 1852 (2017)
97. J.Garousi, H.Honarvar, K.G.Andersson, B.Mitran, A.Orlova, J.Buijs, J.Löfblom, F.Y.Frejd, V.Tolmachev. *Mol. Pharm.*, **13**, 3676 (2016)
98. J.Garousi, F.J.Huizing, A.Vorobyeva, B.Mitran, K.G.Andersson, C.D.Leitao, F.Y.Frejd, J.Löfblom, J.Bussink, A.Orlova, S.Heskamp, V.Tolmachev. *Sci. Rep.*, **9**, 14907 (2019)
99. A.Orlova, H.Wúllberg, S.Stone-Elander, V.Tolmachev. *J. Nucl. Med.*, **50**, 417 (2009)
100. J.Malmberg, M.Sandström, K.Wester, V.Tolmachev, A.Orlova. *Nucl. Med. Biol.*, **38**, 1093 (2011)
101. A.C.Freise, A.M.Wu. *Mol. Immunol.*, **67**, 142 (2015)
102. S.S.Rinne, A.Orlova, V.Tolmachev. *Int. J. Mol. Sci.*, **22**, 3663 (2021)
103. V.Tolmachev, A.Orlova, J.Sörensen. *Semin. Cancer Biol.*, **72**, 185 (2021)
104. J.Nilvebrant, M.Åstrand, M.Georgieva-Kotseva, M.Björnmalm, J.Löfblom, S.Hober. *PLoS One*, **9**, e103094 (2014)
105. J.Garousi, S.Lindbo, J.Nilvebrant, M.Åstrand, J.Buijs, M.Sandström, H.Honarvar, A.Orlova, V.Tolmachev, S.Hober. *Cancer Res.*,**75**, 4364 (2015)
106. S.Lindbo, J.Garousi, M.Åstrand, H.Honarvar, A.Orlova, S.Hober, V.Tolmachev. *Bioconjug. Chem.*, **27**, 716 (2016)
107. S.Lindbo, J.Garousi, B.Mitran, A.Vorobyeva, M.Oroujeni, A.Orlova, S.Hober, V.Tolmachev. *Mol. Pharm.*, **15**, 2674 (2018)
108. J.Garousi, S.Lindbo, J.Borin, E.von Witting, A.Vorobyeva, M.Oroujeni, B.Mitran, A.Orlova, J.Buijs, V.Tolmachev, S.Hober. *Eur. J. Pharm. Biopharm.*, **134**, 37 (2019)
109. V.Tolmachev, E.Mume, S.Sjöberg, F.Y.Frejd, A.Orlova. *Eur. J. Nucl. Med. Mol. Imaging*, **36**, 692 (2009)
110. C.Zahnd, M.Kawe, M.T.Stumpp, C.de Pasquale, R.Tamaskovic, G.Nagy-Davidescu, B.Dreier, R.Schibli, H.K.Binz, R.Waibel, A.Plückthun. *Cancer Res.*, **70**, 1595 (2010)
111. D.Steiner, P.Forrer, A.Plückthun. *J. Mol. Biol.*, **382**, 1211(2008)
112. N.Stefan, P.Martin-Killias, S.Wyss-Stoeckle, A.Honegger, U.Zangemeister-Wittke, A.Plückthun. *J. Mol. Biol.*, **413**, 826 (2011)
113. F.Radom, C.Vonrhein, P.R.E.Mittl, A.Plückthun. *Acta Crystallogr., Sect. F*, **77**, 192 (2021)
114. R.Goldstein, J.Sosabowski, M.Livanos, J.Leyton, K.Vigor, G.Bhavsar, G.Nagy-Davidescu, M.Rashid, E.Miranda, J.Yeung, B.Tolner, A.Plückthun, S.Mather, T.Meyer, K.Chester. *Eur. J. Nucl. Med. Mol. Imaging*, **42**, 288 (2015)
115. A.Vorobyeva, O.Bragina, M.Altai, B.Mitran, A.Orlova, A.Shulga, G.Proshkina, V.Chernov, V.Tolmachev, S.Deyev. *Contrast Media Mol. Imaging*, 6930425 (2018)
116. S.Deyev, A.Vorobyeva, A.Schulga, G.Proshkina, R.Güler, J.Löfblom, B.Mitran, J.Garousi, M.Altai, J.Buijs, V.Chernov, A.Orlova, V.Tolmachev. *Mol. Pharm.*, **16**, 995 (2019)
117. S.M.Deyev, A.Vorobyeva, A.Schulga, A.Abouzayed, T.Günther, J.Garousi, E.Konovalova, H.Ding, T.Gräslund, A.Orlova, V.Tolmachev. *Int. J. Biol. Macromol.*, **145**, 216 (2020)
118. A.Vorobyeva, E.Konovalova, T.Xu, A.Schulga, M.Altai, J.Garousi, S.S.Rinne, A.Orlova, V.Tolmachev, S.Deyev. *Int. J. Mol. Sci.*, **21**, 3310 (2020)
119. A.Vorobyeva, E.Bezverkhniaia, E.Konovalova, A.Schulga, J.Garousi, O.Vorontsova, A.Abouzayed, A.Orlova, S.Deyev, V.Tolmachev. *Molecules*, **25**, 4719 (2020)
120. T.Engfeldt, T.Tran, A.Orlova, C.Widstrìm, J.Feldwisch, L.Abrahmsen, A.Wennborg, A.E.Karlstrìm, V.Tolmachev. *Eur. J. Nucl. Med. Mol. Imaging*, **34**, 1843 (2007)
121. M.Altai, H.Wúllberg, H.Honarvar, J.Strand, A.Orlova, Z.Varasteh, M.Sandström, J.Löfblom, E.Larsson, S.E.Strand, M.Lubberink, S.Ståhl, V.Tolmachev. *J. Nucl. Med.*, **55**, 1842 (2014)
122. J.Sörensen, D.Sandberg, M.Sandström, A.Wennborg, J.Feldwisch, V.Tolmachev, G.Åström, M.Lubberink, U.Garske-Román, J.Carlsson, H.Lindman. *J. Nucl. Med.*, **55**, 730 (2014)
123. J.Sörensen, I.Velikyan, D.Sandberg, A.Wennborg, J.Feldwisch, V.Tolmachev, A.Orlova, Å.Sandström, M.Lubberink, H.Olofsson, J.Carlsson, H.Lindman. *Theranostics*, **6**, 262 (2016)
124. M.Sandström, K.Lindskog, I.Velikyan, A.Wennborg, J.Feldwisch, D.Sandberg, V.Tolmachev, A.Orlova, J.Sörensen, J.Carlsson, H.Lindman, M.Lubberink. *J. Nucl. Med.*, **57**, 867 (2016)
125. O.Bragina, V.Chernov, A.Schulga, E.Konovalova, E.Garbukov, A.Vorobyeva, A.Orlova, L.Tashireva, J.Sorensen, R.Zelchan, A.Medvedeva, S.Deyev, V.Tolmachev. *J. Nucl. Med.*, (2021) (in the press); doi: 10.2967/jnumed.121.262542
126. O.Bragina, E.von Witting, J.Garousi, R.Zelchan, M.Sandström, A.Orlova, A.Medvedeva, A.Doroshenko, A.Vorobyeva, S.Lindbo, J.Borin, N.Tarabanovskaya, J.Sörensen, S.Hober, V.Chernov, V.Tolmachev. *J. Nucl. Med.*, **62**, 493 (2021)
127. A.Vorobyeva, M.Oroujeni, S.Lindbo, S.Hober, T.Xu, Y.Liu, S.S.Rinne, J.Garousi. *Molecules*, **25**, 4448 (2020)
128. M.Altai, J.Garousi, S.S.Rinne, A.Schulga, S.Deyev, A.Vorobyeva. *EJNMMI Res.*, **10**, 7 (2020)
129. J.Garousi, A.Vorobyeva, M.Altai. *Molecules*, **25**, 2673 (2020)
130. V.Tolmachev, A.Orlova, R.Pehrson, J.Galli, B.Baastrup, K.Andersson, M.Sandström, D.Rosik, J.Carlsson, H.Lundqvist, A.Wennborg, F.Y.Nilsson. *Cancer Res.*, **67**, 2773 (2007)

131. A.Orlova, A.Jonsson, D.Rosik, H.Lundqvist, M.Lindborg, L.Abrahmsen, C.Ekblad, F.Y.Frejd, V.Tolmachev. *J. Nucl. Med.*, **54**, 961 (2013)
132. Y.Liu, A.Vorobyeva, T.Xu, A.Orlova, A.Loftenius, T.Bengtsson, P.Jonasson, V.Tolmachev, F.Y.Frejd. *Pharmaceutics*, **13**, 839 (2021)
133. J.Garousi, E.von Witting, J.Borin, A.Vorobyeva, M.Altai, O.Vorontsova, M.W.Konijnenberg, M.Oroujeni, A.Orlova, V.Tolmachev, S.Hober. *Biomaterials*, **266**, 120381 (2021)
134. M.Altai, R.Membreno, B.Cook, V.Tolmachev, B.M.Zeglis. *J. Nucl. Med.*, **58**, 1553 (2017)
135. M.Altai, A.Perols, M.Tsourma, B.Mitran, H.Honarvar, M.Robillard, R.Rossin, W.Hoeve, M.Lubberink, A.Orlova, A.E.Karlström, V.Tolmachev. *J. Nucl. Med.*, **57**, 431 (2016)
136. H.Honarvar, K.Westerlund, M.Altai, M.Sandström, A.Orlova, V.Tolmachev, A.E.Karlström. *Theranostics*, **6**, 93 (2016)
137. K.Westerlund, M.Altai, B.Mitran, M.Konijnenberg, M.Oroujeni, C.Atterby, M.de Jong, A.Orlova, J.Mattsson, P.Micke, A.E.Karlström, V.Tolmachev. *J. Nucl. Med.*, **59**, 1092 (2018)
138. H.Tano, M.Oroujeni, A.Vorobyeva, K.Westerlund, Y.Liu, T.Xu, D.Voncelos, A.Orlova, A.E.Karlström, V.Tolmachev. *Cancers (Basel)*, **13**, 500 (2021)
139. E.J.Postema, C.Frielink, W.J.Oyen, J.M.Raemaekers, D.M.Goldenberg, F.H.Corstens, O.C.Boerman. *Cancer Biother. Radiopharm.*, **18**, 525 (2003)
140. M.J.Koppe, R.P.Bleichrodt, A.C.Soede, A.A.Verhofstad, D.M.Goldenberg, W.J.Oyen, O.C.Boerman. *J. Nucl. Med.*, **45**, 1224 (2004)
141. W.E.Meijs, H.J.Haisma, R.P.Klok, F.B.van Gog, E.Kievit, H.M.Pinedo, J.D.Herscheid. *J. Nucl. Med.*, **38**, 112 (1997)
142. F.B.van Gog, G.W.Visser, J.W.Stroomer, J.C.Roos, G.B.Snow, G.A.van Dongen. *Cancer*, **80**, 2360 (1997)
143. F.Bensch, M.M.Smeenk, S.C.van Es, J.R.de Jong, C.P.Schrìder, S.F.Oosting, M.N.Lub-de Hooge, C.W.Menke-van der Houven van Oordt, A.H.Brouwers, R.Boellaard, E.G.E.de Vries. *Theranostics*, **8**, 4295 (2018)
144. S.Ge, J.Li, Y.Yu, Z.Chen, Y.Yang, L.Zhu, S.Sang, S.Deng. *Molecules*, **26**, 6482 (2021)
145. B.Mitran, V.Tolmachev, A.Orlova. *Curr. Med. Chem.*, **27**, 7090 (2020)
146. S.Lindbo, J.Garousi, B.Mitran, M.Altai, J.Buijs, A.Orlova, S.Hober, V.Tolmachev. *J. Nucl. Med.*, **59**, 93 (2018)
147. J.Chen, S.E.Strand, H.O.Sjögren. *Cancer Biother. Radiopharm.*, **11**, 217 (1996)
148. A.Vorobyeva, A.Schulga, S.S.Rinne, T.Günther, A.Orlova, S.Deyev, V.Tolmachev. *Int. J. Mol. Sci.*, **20**, 3047 (2019)
149. A.Vorobyeva, A.Såhulga, E.Konovalova, R.Güler, B.Mitran, J.Garousi, S.Rinne, J.Löfblom, A.Orlova, S.Deyev, V.Tolmachev. *Int. J. Oncol.*, **54**, 1209 (2019)
150. J.Strand, P.Nordeman, H.Honarvar, M.Altai, A.Orlova, M.Larhed, V.Tolmachev. *ChemistryOpen*, **4**, 174 (2015)
151. R.Waibel, R.Alberto, J.Willuda, R.Finnern, R.Schibli, A.Stichelberger, A.Egli, U.Abram, J.P.Mach, A.Plückthun, P.A.Schubiger. *Nat. Biotechnol.*, **17**, 897 (1999)
152. S.M.Deyev, R.Waibel, E.N.Lebedenko, A.P.Schubiger, A.Plückthun. *Nat. Biotechnol.*, **21**, 1486 (2003)
153. A.Badar, J.Williams, R.T.de Rosales, R.Tavaré, F.Kampmeier, P.J.Blower, G.E.Mullen. *EJNMMI Res.*, **4**, 14 (2014)
154. A.Orlova, F.Y.Nilsson, M.Wikman, C.Widström, S.Ståhl, J.Carlsson, V.Tolmachev. *J. Nucl. Med.*, **47**, 512 (2006)
155. T.Tran, T.Engfeldt, A.Orlova, M.Sandström, J.Feldwisch, L.Abrahmsén, A.Wennborg, V.Tolmachev, A.E.Karlström. *Bioconjug. Chem.*, **18**, 1956 (2007)
156. V.Tolmachev, C.Hofström, J.Malmberg, S.Ahlgren, S.J.Hosseinimehr, M.Sandström, L.Abrahmsén, A.Orlova, T.Gräslund. *Bioconjug. Chem.*, **21**, 2013 (2010)
157. C.Hofström, M.Altai, H.Honarvar, J.Strand, J.Malmberg, S.J.Hosseinimehr, A.Orlova, T.Gräslund, V.Tolmachev. *J. Med. Chem.*, **56**, 4966 (2013)
158. A.Vorobyeva, A.Schulga, E.Konovalova, R.Güler, J.Löfblom, M.Sandström, J.Garousi, V.Chernov, O.Bragina, A.Orlova, V.Tolmachev, S.M.Deyev. *Sci. Rep.*, **9**, 9405 (2019)
159. S.Deyev, G.Proshkina, A.Ryabova, F.Tavanti, M.C.Menziani, G.Eidelshtein, G.Avishai, A.Kotlyar. *Bioconjug. Chem.*, **28**, 2569 (2017)
160. S.Alshehri, S.S.Imam, M.Rizwanullah, S.Akhter, W.Mahdi, M.Kazi, J.Ahmad. *Pharmaceutics*, **13**, 24 (2020)
161. I.V.Balalaeva, T.A.Zdobnova, I.V.Krutova, A.A.Brilkina, E.N.Lebedenko, S.M.Deyev. *J. Biophotonics*, **5**, 860 (2012)
162. T.A.Zdobnova, S.G.Dorofeev, P.N.Tananaev, R.B.Vasiliev, T.G.Balandin, E.F.Edelweiss, O.A.Stremovskiy, I.V.Balalaeva, I.V.Turchin, E.N.Lebedenko, V.P.Zlomanov, S.M.Deyev. *J. Biomed. Opt.*, **14**, 021004 (2009)
163. M.Liu, R.C.Anderson, X.Lan, P.S.Conti, K.Chen. *Med. Res. Rev.*, **40**, 909 (2020)
164. A.N.Generalova, S.V.Sizova, T.A.Zdobnova, M.M.Zarifullina, M.V.Artemyev, A.V.Baranov, V.A.Oleinikov, V.P.Zubov, S.M.Deyev. *Nanomedicine (London)*, **6**, 195 (2011)
165. A.Majkowska-Pilip, W.Gawęda, K.Żelechowska-Matysiak, K.Wawrowicz, A.Bilewicz. *Nanomaterials (Basel)*, **10**, 1366 (2020)
166. P.I.Siafaka, N.Ü.Okur, I.D.Karantas, M.E.Okur, E.A.Gündogdu. *Asian J. Pharm. Sci.*, **16**, 24 (2021)
167. X.Zhang, F.Chen, M.Z.Turker, K.Ma, P.Zanzonico, F.Gallazzi, M.A.Shah, A.R.Prater, U.Wiesner, M.S.Bradbury, M.R.McDevitt, T.P.Quinn. *Biomaterials*, **241**, 119858 (2020)
168. R.M.Pallares, P.Agbo, X.Liu, D.D.An, S.S.Gauny, S.E.Zeltmann, A.M.Minor, R.J.Abergel. *ACS Appl. Mater. Interfaces*, **12**, 40078 (2020)
169. W.Gawçęda, M.Pruszyński, E.Cędrowska, M.Rodak, A.Majkowska-Pilip, D.Gaweł, F.Bruchertseifer, A.Morgenstern, A.Bilewicz. *Nanomaterials (Basel)*, **10**, 2067 (2020)
170. S.Yook, Z.Cai, J.J.Jeong, Y.Lu, M.A.Winnik, J.P.Pignol, R.M.Reilly. *Mol. Pharm.*, **17**, 1226 (2020)
171. V.O.Shipunova, E.N.Komedchikova, P.A.Kotelnikova, I.V.Zelepukin, A.A.Schulga, G.M.Proshkina, E.I.Shramova, H.L.Kutscher, G.B.Telegin, A.V.Kabashin, P.N.Prasad, S.M.Deyev. *ACS Nano*, **14**, 12781 (2020)
172. X.Xu, C.Han, C.Zhang, D.Yan, C.Ren, L.Kong. *Theranostics*, **11**, 6477 (2021)
173. O.N.Shilova, S.M.Deyev. *Acta Naturae*, **11**, 42 (2019)
174. D.Zheng, C.Wan, H.Yang, L.Xu, Q.Dong, C.Du, J.Du, F.Li. *Int. J. Nanomed.*, **15**, 10007 (2020)
175. S.Huang, L.Zhang, M.Xu, C.Li, H.Fu, J.Huang, X.Jin, S.Liang, H.Wang. *Adv. Health Mater.*, **10**, e2001029 (2021)
176. E.L.Guryev, N.O.Volodina, N.Y.Shilyagina, S.V.Gudkov, I.V.Balalaeva, A.B.Volovetskiy, A.V.Lyubeshkin, A.V.Sen', S.A.Ermilov, V.A.Vodeneev, R.V.Petrov, A.V.Zvyagin, Z.I.Alferov, S.M.Deyev. *Proc. Natl. Acad. Sci. USA*, **115**, 9690 (2018)
177. S.Y.Fam, C.F.Chee, C.Y.Yong, K.L.Ho, A.R.Mariatulqabtiah, W.S.Tan. *Nanomaterials (Basel)*, **10**, 787 (2020)
178. Y.Liu, Z.Wang, Y.Liu, G.Zhu, O.Jacobson, X.Fu, R.Bai, X.Lin, N.Lu, X.Yang, W.Fan, J.Song, Z.Wang, G.Yu, F.Zhang, H.Kalish, G.Niu, Z.Nie, X.Chen. *ACS Nano*, **11**, 10539 (2017)
179. M.P.Nikitin, I.V.Zelepukin, V.O.Shipunova, I.L.Sokolov, S.M.Deyev, P.I.Nikitin. *Nat. Biomed. Eng.*, **4**, 717 (2020)
180. I.V.Zelepukin, A.V.Yaremenko, M.V.Yuryev, A.B.Mirkasymov, I.L.Sokolov, S.M.Deyev, P.I.Nikitin, M.P.Nikitin. *J. Control. Release*, **326**, 181 (2020)

181. A.B.Mirkasymov, I.V.Zelepukin, P.I.Nikitin, M.P.Nikitin, S.M.Deyev. *J. Control. Release*, **330**, 111 (2021)
182. I.V.Zelepukin, A.V.Yaremenko, I.N.Ivanov, M.V.Yuryev, V.R.Cherkasov, S.M.Deyev, P.I.Nikitin, M.P.Nikitin. *ACS Nano*, **15**, 11341 (2021)
183. I.Beyer, H.Cao, J.Persson, H.Song, M.Richter, Q.Feng, R.Yumul, R.van Rensburg, Z.Li, R.Berenson, D.Carter, S.Roffler, C.Drescher, A.Lieber. *Clin. Cancer. Res.*, **18**, 3340 (2012)
184. I.Beyer, R.van Rensburg, A.Lieber. *Tissue Barriers*, **1**, e23647 (2013)
185. R.Pitner, J.Kim, J.Davis-Bergthold, C.Turner, E.Vassal-Stermann, H.Wang, J.Adams, L.Carter, J.A.Ahlgren, P.Fender, A.Lieber, D.Carter, S.A.Gray. *Sci. Rep.*, **9**, 6169 (2019)
186. O.Shilova, E.Shramova, G.Proshkina, S.Deyev. *Int. J. Mol. Sci.*, **22**, 4975 (2021)
187. O.N.Shilova, E.S.Shilov, A.Lieber, S.M.Deyev. *J. Control. Release*, **286**, 125 (2018)
188. C.E.Wang, R.C.Yumul, J.Lin, Y.Cheng, A.Lieber, S.H.Pun. *J. Control. Release*, **272**, 9 (2018)
189. K.Gordon, I.Gulidov, A.Semenov, O.Golovanova, S.Koryakin, T.Makeenkova, S.Ivanov, A.Kaprin. *Rep. Pract. Oncol. Radiother.*, **26**, 203 (2021)
190. A.S.Sobolev. *Acta Naturae*, **12**, 47 (2020)
191. A.A.Rosenkranz, T.A.Slastnikova, G.P.Georgiev, M.R.Zalutsky, A.S.Sobolev. *Nucl. Med. Biol.*, **80**–**81**, 45 (2020)